Journal of Materials Chemistry C

PAPER

View Article Online
View Journal | View Issue

Cite this: J. Mater. Chem. C, 2014, 2, 9720

trans-Bis(alkylphosphine) platinum(II)-alkynyl complexes showing broadband visible light absorption and long-lived triplet excited states†

Huiru Jia,[a] Betül Küçüköz,[b] Yongheng Xing,[c] Poulomi Majumdar,[a] Caishun Zhang,[a] Ahmet Karatay,[b] Gul Yaglioglu,[b] Ayhan Elmali,[b] Jianzhang Zhao*[a] and Mustafa Hayvali*[d]

Received 29th July 2014
Accepted 10th September 2014

DOI: 10.1039/c4tc01675k

www.rsc.org/MaterialsC

Heteroleptic *trans*-bis(alkylphosphine) platinum(II) bisacetylide complexes **Pt-1** and **Pt-2** were prepared to achieve *broadband* absorption of visible light. Two different ethynylBodipy ligands, 2-ethynylBodipy and 2,6-diethynylBodipy or 8-(4′-ethynylphenyl)Bodipy, were used in each complex. Each Bodipy ligand gives strong absorption in the visible spectral region, but at different wavelengths, thus broadband absorption in the visible spectral region was achieved for the Pt(II) complexes (ε is up to 1.85 $\times$ 10^5 M^{-1} cm^{-1} in the region of 450–700 nm). Singlet energy transfer from the peripheral coordinated Bodipy to the central coordinated Bodipy (with 2,6-diethynyl substitution) was confirmed by steady state absorption/luminescence spectroscopy, fluorescence excitation spectroscopy and nanosecond/femtosecond ultrafast time-resolved transient absorption spectroscopy. Long-lived triplet excited states were observed for both complexes (τ_T = 63.13 μs for **Pt-1** and τ_T = 94.18 μs for **Pt-2**). Nanosecond time-resolved transient absorption spectroscopy indicated that the triplet excited state of **Pt-1** is distributed on *both* Bodipy units. For **Pt-2**, however, the T_1 state is confined to the central coordinated Bodipy ligand. These complexes show high singlet oxygen ($^1O_2$) quantum yields (Φ_Δ = 76.0%). With nanosecond pulsed laser excitation, delayed fluorescence was observed for the complexes (τ_{DF} = 43.8 μs for **Pt-1** and τ_{DF} = 111.0 μs for **Pt-2**), which is rarely reported for transition metal complexes. The complexes were used as efficient multi-wavelength excitable triplet photosensitizers for triplet–triplet annihilation upconversion.

Introduction

Transition metal complexes have been used in photocatalysis, hydrogen production (H_2), photoredox catalytic organic reactions, molecular devices, photodynamic therapy (PDT), nonlinear optics, and electroluminescence,[1–13] as well as in photochemistry studies, such as investigations of singlet or triplet exciton migration.[14–16] Concerning these aspects, the Pt(II) complexes are of particular interest because of the efficient production of triplet excited states and the readily derivatizable molecular structures.[17,18] Since most of the applications of these complexes are related to the triplet excited states, with which the consequential electron transfer or triplet energy transfer is initiated, the visible light harvesting ability and the lifetime of the T_1 state of these complexes are crucial, because the above-mentioned *intermolecular* processes are capable of being enhanced with the abundant molecules at the excited states and the long-living triplet excited states. The weak absorption of conventional transition metal complexes may be attributed to the weakly allowed $S_0 \rightarrow {}^1$MLCT transition (charge transfer character).[13] The visible light-absorbing ability is capable of being enhanced by switching the $S_0 \rightarrow S_1$ transition to the $S_0 \rightarrow {}^1$IL (intraligand) transition, with the latter as a strongly allowed π–π* transition. In recent years Pt(II) complexes with visible light-harvesting ligands were reported.[5,11] Our group reported Pt(II) complexes which contain visible light-harvesting ligands such as Bodipy, coumarin, naphthalenediimide, perylene bisimide, *etc.*[13] These complexes show strong visible light absorption and long-lived triplet excited states, and have been used in triplet–triplet annihilation (TTA) upconversion,

[a]State Key Laboratory of Fine Chemicals, School of Chemical Engineering, Dalian University of Technology, E-208 West Campus, 2 Ling Gong Rd, Dalian 116024, P. R. China. E-mail: zhaojzh@dlut.edu.cn; Web: http://finechem.dlut.edu.cn/photochem

[b]Department of Engineering Physics, Faculty of Engineering, Ankara University, 06100 Beşevler, Ankara, Turkey

[c]College of Chemistry and Chemical Engineering, Liaoning Normal University, No. 850 Huanghe Road, Dalian 116029, P.R. China

[d]Department of Chemistry, Faculty of Science, Ankara University, 06100 Beşevler, Ankara, Turkey. E-mail: hayvali@science.ankara.edu.tr

† Electronic supplementary information (ESI) available. CCDC 973944. For ESI and crystallographic data in CIF or other electronic format see DOI: 10.1039/c4tc01675k

photoredox catalytic organic reactions and photosensitization of singlet oxygen ($^1O_2$).[13]

We noted that a common disadvantage of these complexes is left to overcome, that is, there is usually only a single kind of visible light-harvesting ligand in these complexes, as a result, there is only *one* major absorption band in the visible spectral region.[5,13,17] This is clearly a drawback if a panchromatic light source was used, such as solar light. Therefore, it is important to prepare Pt(II) complexes that show broadband absorption of visible light. This goal cannot be achieved by using the conventional molecular structural protocol based on using a single kind of visible light-harvesting ligand in the complex molecule.[13]

On the other hand, the *trans*-bis(alkylphosphine) platinum(II)-alkynyl complexes have attracted much attention.[5,19–24] The molecular structure of these compounds can be easily modified by using different acetylide ligands, providing tunability of both the photophysical and redox properties.[1,19] However, *trans*-bis(alkylphosphine) platinum(II)-alkynyl complexes showing strong visible light absorption were rarely reported.[20,25,26] We have shown the rich triplet excited state-related photochemistry of organic fluorophores, such as Bodipy, coumarin, rhodamine, NDI and **PBI** with transition metal complexes,[13] thus it is interesting to study the intramolecular excited state energy transfer with the *trans*-bis(alkylphosphine) platinum(II)-alkynyl complexes that contain organic chromophores.

In organic molecular dyads, fluorescence resonance energy transfer (FRET) was very often used to achieve a *broadband* visible light absorption.[27] However, to the best of our knowledge, this strategy was rarely used to achieve broadband visible light absorption in transition metal complexes.[13,17,18] Recently we prepared a Pt(II) complex with Bodipy and naphthalenediimide ligands, but the absorption wavelength and intensity are not satisfactory.[19]

In this paper we propose a strategy to achieve *broadband* visible light-absorption in transitional metal complexes. Our method is exemplified with two heteroleptic *trans*-bis(alkylphosphine) platinum(II)-alkynyl complexes (**Pt-1** and **Pt-2**, Scheme 1).[5,19–24] For transition metal complexes containing multi-chromophores to achieve broadband absorption of visible light, it is important to control the direction of the singlet energy transfer so that the spin converter acts as the singlet energy acceptor to ensure efficient transformation of the photoexcitation energy into triplet state energy.[13b,28,29]

Herein we prepared two heteroleptic *trans*-bis(alkylphosphine) platinum(II)-alkynyl complexes (**Pt-1** and **Pt-2**, Scheme 1). In these complexes, different Bodipy units are connected to the Pt(II) atom either at the 2-position or the *meso*(4′-phenyl) position of the Bodipy unit, so that different absorption wavelengths and T_1 state energy levels resulted, and intramolecular RET is ensured with the central 2,6-coordinated Bodipy moiety as the singlet energy acceptor, which is an efficient spin converter to produce triplet excited states.[13b]

With steady state and nanosecond or femtosecond ultrafast time-resolved transient absorption spectroscopy techniques, we confirmed the singlet and triplet excited state energy transfer in these complexes. By nanosecond time-resolved transient absorption spectroscopy, we found that the triplet excited state of **Pt-1** is *delocalized* on the three Bodipy ligands, due to degenerated T_1 and T_2 states, whereas in **Pt-2** the triplet excited state is exclusively confined to one Bodipy ligand. Long-lived triplet excited states (τ_T is up to 94.18 μs) were observed for the complexes. The complexes were used as multi-wavelength excitable triplet photosensitizers for TTA upconversion.

Experimental section

Analytical measurements

All the chemicals used in synthesis were analytically pure and were used as received. Solvents were dried and distilled before synthesis. *cis*-Pt[P(*n*-Bu)$_3$]$_2$Cl$_2$ was prepared according to a literature method,[5] and the synthesis of compounds **1**, **2**, and **3** was reported previously.[30,31]

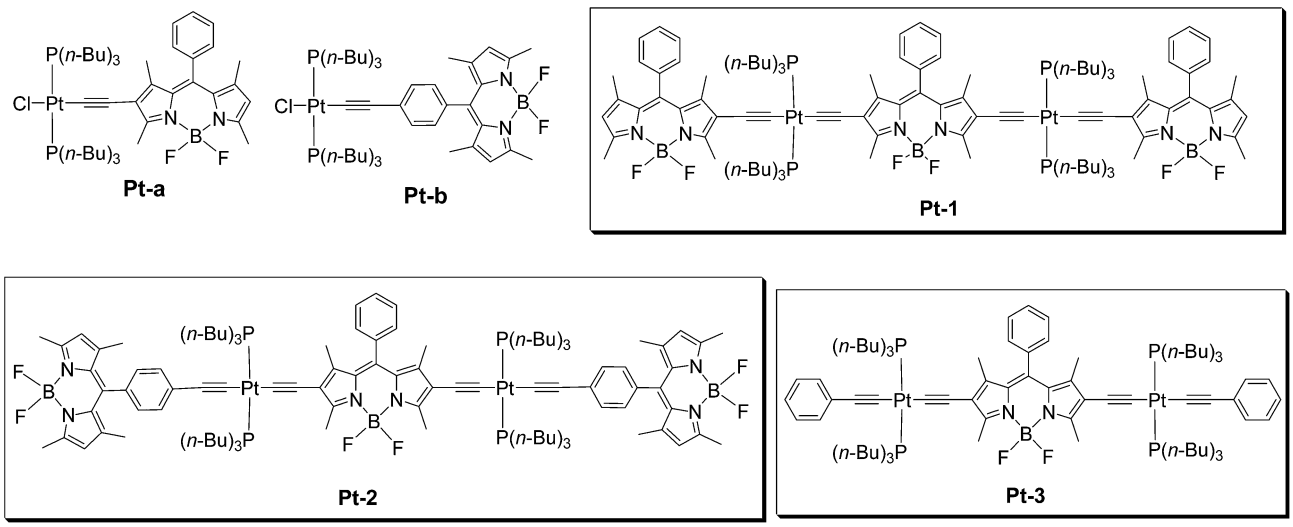

Scheme 1 Pt(II) complexes used in the study. The known complex **Pt-3** is also presented.

Complex Pt-a. Under an Ar atmosphere, compound **1** (34.8 mg, 0.1 mmol) and *cis*-Pt[P(*n*-Bu)$_3$]$_2$Cl$_2$ (80 mg, 0.12 mmol) were dissolved in a mixed solvent of THF/Et$_2$NH (1 : 1, v/v, 6 mL), and the flask was placed in a Dewar flask (ethyl acetate/liquid nitrogen low temperature bath). The flask was evacuated and back-filled with Ar. Then CuI (3.8 mg, 0.02 mmol) was added. The temperature of the mixture was allowed to rise from −78 °C to RT within 8 hours. Then deionized water was used to quench the reaction. The mixture was extracted with dichloromethane (**DCM**, 3 × 15 mL). The organic layer was dried over anhydrous Na_2SO_4, filtered and the solvent was removed under reduced pressure. The crude product was purified using column chromatography (silica gel, CH_2Cl_2 : petroleum ether = 1 : 2, v/v) to give compound **Pt-a** as a purple solid. Yield: 44.5 mg (45.3%). M.p.: 89.9–91.5 °C. ^{1}H NMR (400 MHz, $CDCl_3$): 7.48–7.28 (m, 5H), 5.93 (s, 1H), 2.64 (s, 3H), 2.53 (s, 1H), 1.93 (s, 12H), 1.43–1.35 (m, 30H), 0.89 (t, 18H, J = 8.0 Hz). ^{13}C NMR (100 MHz, $CDCl_3$): δ 158.4, 154.1, 142.0, 140.9, 140.7, 135.5, 131.5, 131.1, 129.2, 129.0, 128.2, 122.2, 120.7, 92.0, 90.0, 29.9, 26.3, 24.4, 22.2, 22.1, 21.9, 14.4, 14.0, 13.3. MALDI-HRMS: calcd ([$C_{45}H_{72}BClF_2N_2P_2Pt$]$^+$), m/z = 981.4568, found, m/z = 981.4590. Anal. calcd for [$C_{45}H_{72}BClF_2N_2P_2Pt$] + 1.6$C_6H_{14}$]: C, 58.50; H, 8.48; N, 2.50. Found: C, 58.79; H, 8.09; N, 2.31.

Complex Pt-b. Under an Ar atmosphere, compound **2** (34.8 mg, 0.1 mmol) and *cis*-Pt[P(*n*-Bu)$_3$]$_2$Cl$_2$ (79.6 mg, 0.12 mmol) were dissolved in Et$_2$NH (8 mL), and the flask was evacuated and back-filled with Ar for several times. The mixture was heated at 45 °C for 9 h. The solvent was removed under reduced pressure. The crude product was further purified using column chromatography (silica gel, CH_2Cl_2 : petroleum ether = 1 : 1, v/v) to give **Pt-b** as a yellow solid. Yield: 36.9 mg (37.6%). M.p.: 118.6–120.4 °C. ^{1}H NMR (400 MHz, $CDCl_3$): 7.35–7.08 (m, 4H), 5.97 (s, 2H), 2.55 (s, 6H), 2.04 (s, 12H), 1.59 (m, 12H), 1.49–1.40 (m, 18H), 0.92 (t, 18H, J = 8.0 Hz). ^{13}C NMR (100 MHz, $CDCl_3$): δ 155.4, 143.3, 142.3, 131.6, 129.8, 127.7, 121.2, 106.2, 86.2, 86.0, 85.9, 29.9, 26.3, 24.6, 24.5, 24.4, 22.4, 22.3, 22.1, 14.7, 13.9. MALDI-HRMS: calcd ([$C_{45}H_{72}BClF_2N_2P_2Pt$]$^+$), m/z = 981.4568, found, m/z = 981.4578. Anal. calcd for [$C_{45}H_{72}BClF_2N_2P_2Pt$] + 0.6$C_6H_{14}$ + 0.3CH_2Cl_2]: C, 55.43; H, 7.71; N, 2.64. Found: C, 55.45; H, 7.44; N, 2.49.

Complex Pt-1. Under an Ar atmosphere, compounds **Pt-a** (24.5 mg, 0.025 mmol) and **3** (4.6 mg, 0.0125 mmol) were dissolved in a mixed solvent of THF/Et$_2$NH (3 mL/3 mL), and the flask was evacuated and back-filled with Ar several times. CuI (3.0 mg, 0.015 mmol) was added, and the mixture was stirred at 0–5 °C for 1 h. Deionized water was used to quench the reaction. The mixture was extracted with **DCM** (3 × 15 mL). The combined organic layer was dried over Na_2SO_4, filtered and the solvent was removed under reduced pressure. The crude product was purified using column chromatography (silica gel, CH_2Cl_2 : petroleum ether = 1 : 1, v/v) to give complex **Pt-1** as a dark blue solid. Yield: 17.7 mg (62.5%). M.p.: >250 °C. ^{1}H NMR (400 MHz, $CDCl_3$): 7.47–7.27 (m, 12H), 5.91 (s, 2H), 2.64–2.61 (d, 12H, J = 12.0 Hz), 1.39–1.33 (m, 66H), 2.52 (s, 6H), 0.84 (t, 36H, J = 8.0 Hz). ^{13}C NMR (100 MHz, $CDCl_3$): δ 159.1, 157.1, 153.5, 141.5, 141.0, 140.5, 139.9, 139.5, 135.8, 135.5, 131.3, 130.9, 128.9, 128.2, 122.5, 121.5, 120.4, 115.7, 114.4, 100.0, 99.7, 29.9, 26.5, 24.5, 24.42, 24.36, 23.9, 23.8, 23.6, 14.4, 14.0, 13.5, 13.4. MALDI-HRMS: calcd ([$C_{113}H_{161}B_3F_6N_6P_4Pt_2$]$^+$), m/z = 2263.1212, found, m/z = 2263.1389. Anal. calcd for [$C_{113}H_{161}B_3F_6N_6P_4Pt_2$ + C_6H_{14}]: C, 60.82; H, 7.51; N, 3.58. Found: C, 60.79; H, 7.24; N, 3.38.

Complex Pt-2. Complex **Pt-2** was prepared by a procedure similar to that for complex **Pt-1**, with **Pt-b** (29.0 mg, 0.03 mmol) as the starting material, instead of **Pt-a**. Complex **Pt-2** was obtained as a dark green solid. Yield: 12.0 mg (33.3%). M.p.: 226.4–228.6 °C. ^{1}H NMR (400 MHz, $CDCl_3$): δ 7.49–7.48 (m, 3H), 7.36 (d, J = 10.0 Hz, 4H), 7.29–7.27 (m, 2H), 7.08 (d, J = 10.0 Hz, 4H), 5.97 (s, 4H), 2.64 (s, 6H), 2.55 (s, 12H), 2.13–2.08 (m, 24H), 1.61–1.55 (m, 24H), 1.45 (s, 12H), 1.43–1.37 (m, 30H), 0.89 (t, J = 10 Hz, 36H). ^{13}C NMR (100 MHz): 159.1, 157.5, 145.8, 144.9, 142.2, 142.0, 137.8, 133.7, 133.3, 133.1, 132.3, 131.3, 131.1, 130.6, 123.3, 117.3, 117.1, 117.0, 113.3, 113.2, 113.1, 111.0, 102.0, 32.1, 28.7, 26.7, 26.6, 26.4, 26.3, 26.1, 16.7, 15.9, 15.4. MALDI-HRMS: calcd ([$C_{113}H_{161}B_3F_6N_6P_4Pt_2$]$^+$), m/z = 2263.1212, found, m/z = 2263.1409. Anal. calcd for [$C_{113}H_{161}B_3F_6N_6P_4Pt_2$]: C, 59.95; H, 7.17; N, 3.71. Found: C, 60.05; H, 6.87; N, 3.87.

Crystal structure. The crystal was mounted on glass fibers for X-ray measurement. Reflection data were collected at room temperature on a Bruker AXS SMART APEX II CCD diffractometer with graphite-monochromatized Mo-Kα radiation (λ = 0.71073 Å) and a ω scan mode. All the measured independent reflections ($I > 2\sigma(I)$) were used in the structural analyses, and semi-empirical absorption corrections were applied using the SADABS program. The structures were solved by the direct method using SHELXL-97. The hydrogen atoms of the organic frameworks were fixed at calculated positions geometrically and refined by using a riding model. In particular, the atoms (C22–C45) of the ligand are found to be disordered and modelled over two split positions with occupancies in a ratio of 0.3 : 0.7. All corresponding non-hydrogen atoms were refined by using the "Sadi" and "Simu" restraints to make the parameters of the disordered atoms more reasonable. A single crystal of **Pt-b** suitable for X-ray diffraction was grown by layering *n*-hexane onto the dichloromethane solution of the complex. The ORTEP drawing of **Pt-b** is depicted in Fig. 1. Selected atomic distances and bonding angles are summarized in Table 1.†

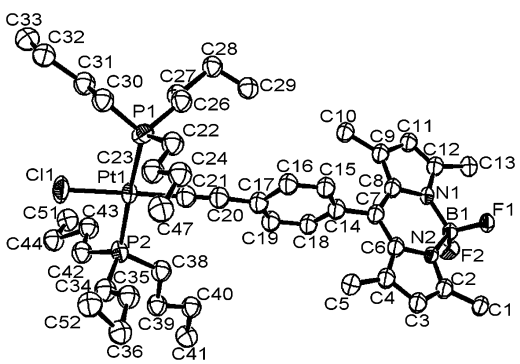

Fig. 1 The ORTEP view of the single crystal structure of **Pt-b** with 35% thermal ellipsoids.

Table 1 Selected bond lengths (Å) and the angles (°) for complex **Pt-b**

Bond lengths (Å)		Bond angles (°)	
Pt(1)–C(21)	1.965(7)	Cl(1)–Pt(1)–C(21)	178.2(2)
Pt(1)–Cl(1)	2.358(3)	Cl(1)–Pt(1)–P(1)	93.6(1)
Pt(1)–P(1)	2.318(2)	Cl(1)–Pt(1)–P(2)	88.54(9)
Pt(1)–P(2)	2.294(2)	P(1)–Pt(1)–P(2)	175.69(9)
C(20)–C(21)	1.18(1)	P(1)–Pt(1)–C(21)	86.2(2)
		P(2)–Pt(1)–C(21)	91.6(2)

Nanosecond time-resolved transient difference absorption spectroscopy. Nanosecond time-resolved transient difference absorption spectra were recorded on a LP920 laser flash photolysis spectrometer (Edinburgh Instruments, Livingston, UK). The sample solution was purged with N_2 or argon for 30 min before measurement. The samples were excited with a nanosecond pulsed laser (Vibrant 355II, wavelength tunable in the range of 410–2400 nm), and the transient signals were recorded on a Tektronix TDS 3012B oscilloscope.

Femtosecond ultrafast transient difference absorption spectroscopy. The ultrafast wavelength dependent pump probe spectroscopy measurements were performed using a Ti:sapphire laser amplifier-optical parametric amplifier system (Spectra Physics, Spitfire Pro XP, TOPAS) and a commercial setup (Spectra Physics, Helios). Pulse duration was measured to be 100 fs. Wavelengths of the pump beam were chosen according to the absorption spectra of complex **Pt-2** as 500 nm (selective excitation into the peripheral Bodipy moiety) and 640 nm (selective excitation into the central coordinated Bodipy moiety). White light continuum was used as a probe beam.

TTA upconversion. A diode-pumped solid state continuous laser was used for upconversion (632 nm and 589 nm). The laser power was measured with a phototube. The mixed solution of the Pt(II) complex (triplet photosensitizers) and **PBI** (triplet acceptor) was degassed for at least 15 min with N_2 or argon before measurement. The spectra were recorded on an adapted RF5301PC spectrofluorometer (Shimadzu, Japan).

The delayed fluorescence of the upconversion (τ_{DF}). The delayed fluorescence lifetimes (τ_{DF}) and spectra were recorded with an Opolette™ 355II + UV nanosecond pulsed laser (typical pulse length: 7 ns, pulse repetition: 20 Hz, peak OPO energy: 4 mJ, and wavelength is tunable in the range of 210–355 nm and 410–2200 nm. OPOTEK, USA), which is synchronized to a FLS 920 spectrofluorometer (Edinburgh, U.K.). The decay kinetics of the upconverted fluorescence (delayed fluorescence) was monitored with a FLS 920 spectrofluorometer (Edinburgh Instruments, Livingston, UK). The prompt fluorescence lifetime of the triplet acceptor perylene was measured with an EPL picosecond pulsed laser (405 nm) which is synchronized to the FLS 920 spectrofluorometer.

Results and discussion

Molecule design and synthesis

The principal molecular designing strategy of heteroleptic **Pt-1** and **Pt-2** is to use different Bodipy ligands showing different absorption wavelengths, in *one* Pt(II) complex molecule. Moreover, the energy acceptor acts as the spin converter,[13b] thus to convert the harvested excitation energy to the triplet state. Bodipy was selected as the visible light harvesting chromophore because of its strong absorption of visible light, high fluorescence quantum yields and easiness of derivatization.[32–39] High fluorescence quantum yield indicates that the internal conversion is weak and it is more likely the ISC will be efficient if the Bodipy is attached to the Pt(II) centre. The Bodipy ligands in the complex molecule are with different coordination profiles, either at the 2-position of the π-core of Bodipy, or the 4′-position of the *meso*-phenyl group (Scheme 1). Thus the two coordination moieties give different absorption wavelengths.[12,13]

The central coordinated Bodipy units with 2,6-diethynyl presumably will show a longer absorption wavelength than the peripheral Bodipy ligands, which are metalated at the 2-position (**Pt-1**), or at the 4′-position of the *meso*-phenyl group of the Bodipy unit (**Pt-2**). Thus with spectral overlap, singlet energy transfer from the peripheral coordinated Bodipy ligands to the central coordinated Bodipy ligand is envisaged. With the central coordinated Bodipy moiety as the efficient spin converter to produce triplet excited states, *effective* broadband absorption was achieved for **Pt-1** and **Pt-2**. The central coordinated Bodipy unit and the peripheral coordinated Bodipy at the 2-position (**Pt-1**) are expected to undergo efficient ISC because the metalation is directly on the π-core of the Bodipy chromophore.[13]

In **Pt-2**, the metalation of the peripheral Bodipy unit is on the *meso*-phenyl moiety, not on the π-core of the Bodipy. As a result, the UV-vis absorption of this ligand is not perturbed, *i.e.* it is at *ca.* 500 nm and the emission band overlaps with the absorption spectra of the central coordinated Bodipy unit. Thus singlet energy transfer from the peripheral Bodipy unit to the central Bodipy unit is expected. Complexes **Pt-a** and **Pt-b** were prepared as reference complexes. The previously reported **Pt-3** was used as a reference for photophysical studies.

The preparation of the ligands is with Bodipy as the starting material (Scheme 2). Iodination and the Sonogashira coupling reactions readily introduce either mono- or bis-acetyl units at the 2- and 6-positions of the Bodipy chromophore. The Bodipy ligand with the ethynyl group at the *meso*-position was prepared with 4-bromobenzenaldehyde.

Complexes **Pt-a** and **Pt-b** are the synthons for complexes **Pt-1** and **Pt-2** (Scheme 2). CuI catalyzed acetylization readily gives the desired complexes **Pt-1** and **Pt-2** with moderate to satisfactory yields. The reference complexes **Pt-a** and **Pt-b** were prepared by similar methods. All the complexes were fully characterized by ^{1}H NMR, ^{13}C NMR and HR MS.

Single crystal molecular structures

The single crystal structure of complex **Pt-b** was determined (Fig. 1). The coordination geometry of the Pt(II) center is square planar with two PBu_3 ligands, an ethynyl ligand and a Cl atom in a *trans*-arrangement.[40] The *meso*-phenyl moiety takes a perpendicular geometry toward the π-core of the Bodipy chromophore. Thus there is no efficient π-conjugation across this phenyl group. This postulation was confirmed by the unchanged UV-vis

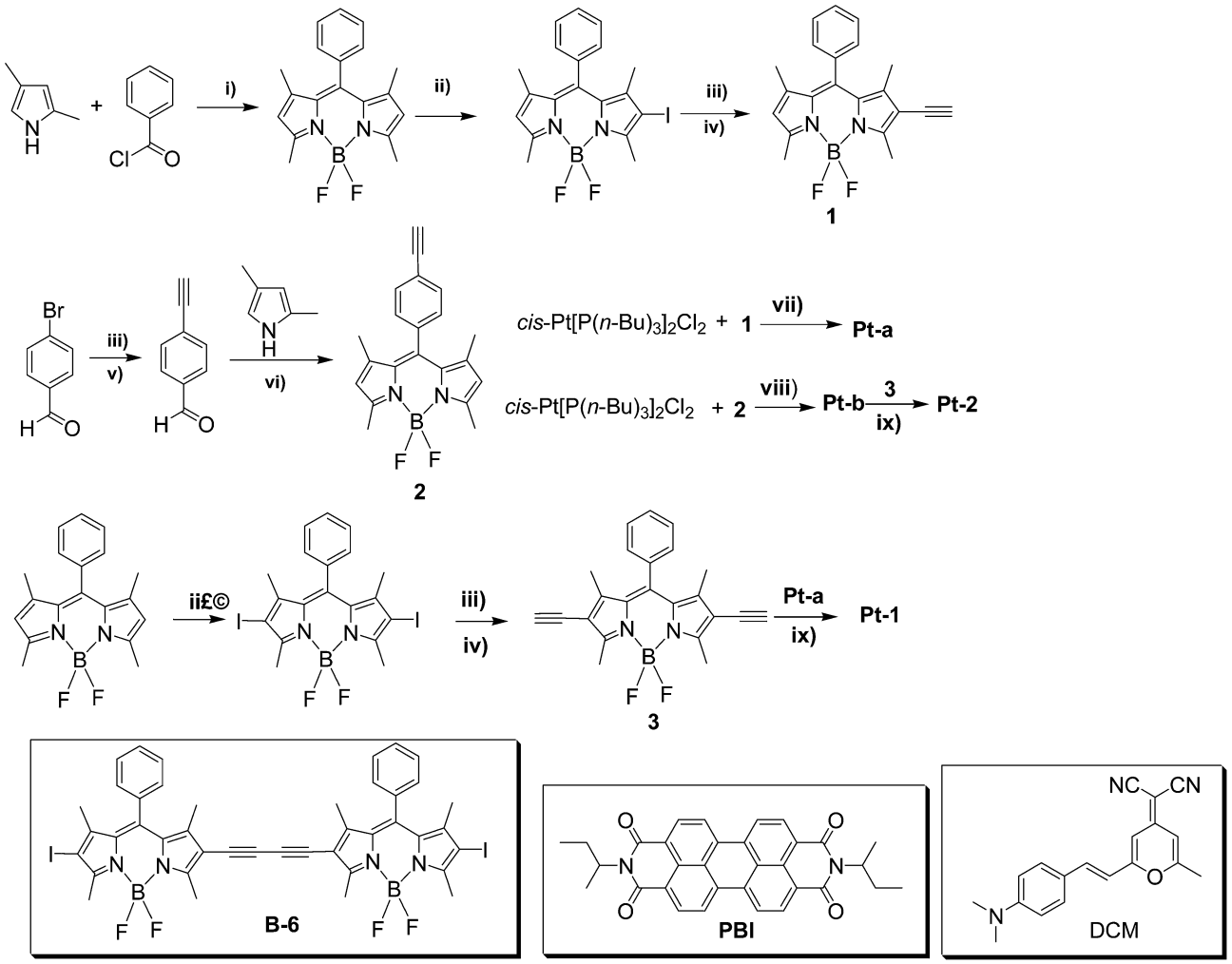

Scheme 2 Preparation of the ligands and the Pt(II) complexes. The model complex **Pt-3**, triplet acceptor **PBI** used in TTA upconversion and the standards (**B-6** and **DCM**) for determination of the fluorescence quantum yields are also presented. Reagents and conditions: (i) dry CH_2Cl_2, $BF_3{\cdot}OEt_2$, NEt_3; (ii) NIS, RT; (iii) trimethylsilylacetylene, $Pd(PPh_3)_2Cl_2$, PPh_3, CuI, NEt_3, reflux, 8 h; (iv) Bu_4NF, THF, −78 °C; (v) K_2CO_3, MeOH, RT, 3 h; (vi) dry CH_2Cl_2, CF_3COOH, $BF_3{\cdot}OEt_2$, NEt_3; (vii) distilled THF, $NHEt_2$, CuI, −78 °C to RT, 8 h; (viii) $NHEt_2$, 45 °C, 8 h; (ix) THF/$HNEt_2$, CuI, 0–5 °C.

absorption of the Bodipy unit upon coordination with the Pt(II) center in complex **Pt-b**. The C(21)–Pt(1) bond length is 1.965 Å. The P(1)–Pt(1) bond length is 2.318 Å. The C≡C bond length, C(21)–C(20), is 1.18 Å. All these bond lengths are similar to the reported linear Pt(II) complexes.[41]

Redox properties

The redox properties of the complexes were studied (Fig. 2). Complex **Pt-a** shows reversible oxidation wave at $E_{1/2} = +0.62$ V, and a reversible reduction wave at $E_{1/2} = -1.52$ V (Fig. 2a). The reversible reduction potential of **Pt-b** is at −1.51 V (Fig. 2b), which is similar to **Pt-a**. Irreversible oxidation wave at +0.91 V was observed for **Pt-b**. The energy gap of **Pt-a** is smaller than that of complex **Pt-b**. These differences can be attributed to the different linkage between the Pt(II) coordination centre and the Bodipy chromophore in complexes **Pt-a** and **Pt-b**.[13] The cathodically shifted oxidation wave of complex **Pt-a** as compared with **Pt-b** may be due to the π-backbonding in **Pt-a**, for which the π-conjugation core of the Bodipy moiety is connected to the coordination centre.

The redox potentials of complex **Pt-1** were studied (Fig. 2c). A reversible reduction wave was observed at $E_{1/2} = -1.56$ V. By comparison with the redox potential of **Pt-3**, the reduction wave at −1.56 V can be attributed to the sum of complexes **Pt-a** and **Pt-1**. A reversible oxidation wave at $E_{1/2} = +0.43$ V was observed. By comparison with **Pt-3**, this wave can be attributed to the central coordination Bodipy moiety. The oxidation wave of the peripherally coordinated Bodipy moiety in **Pt-1** is at +0.70 V, which is anodically shifted as compared with that of complex **Pt-a**. This change can be attributed to the weaker π-backbonding in **Pt-1** than in complex **Pt-a**. Similar results were observed for complex **Pt-2** (Fig. 2d). Generally the redox potentials of the complexes **Pt-1** and **Pt-2** are the sum of the central coordinated Bodipy moiety and the respective peripheral coordinated Bodipy units (Table 2). Therefore, there is no strong electronic interaction, such as π-conjugation, between the chromophores in **Pt-1** and **Pt-2** at ground

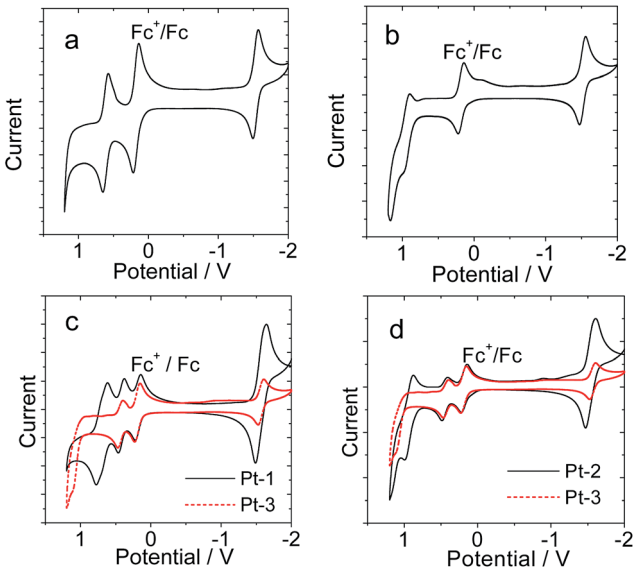

Fig. 2 Cyclic voltammogram of the complexes. (a) **Pt-a**, (b) **Pt-b**, (c) **Pt-1**, and (d) **Pt-2**. The data of **Pt-3** are presented in (c) and (d) for comparison. Ferrocene (Fc) was used as an internal reference ($E_{1/2}$ = +0.64 V (Fc^+/Fc) *vs.* standard hydrogen electrode). In deaerated CH_2Cl_2 containing 0.5 mM photosensitizers with ferrocene, 0.10 M Bu_4NPF_6 as a supporting electrolyte, and $Ag/AgNO_3$ a reference electrode. Scan rates: 100 mV s^{-1} 20 °C.

Table 2 Electrochemical data of Pt(II) complexes[a]

Compound	Oxidation (V)	Reduction (V)
Pt-a	+0.62	−1.52
Pt-b	+0.91	−1.51
Pt-1	+0.43, +0.70	−1.56
Pt-2	+0.45, +0.93	−1.54
Pt-3	+0.44	−1.56

[a] Cyclic voltammetry in Ar saturated CH_2Cl_2 containing 0.10 M Bu_4NPF_6 as a supporting electrolyte; counter electrode as the Pt electrode; working electrode as the glassy carbon electrode; $Ag/AgNO_3$ couple as the reference electrode. c [Ag^+] = 0.1 M. 0.5 mM photosensitizers in CH_2Cl_2, 25 °C.

states. This conclusion is supported by the UV-vis absorption and the luminescence studies.

Steady-state electronic spectroscopy (UV-vis absorption and luminescence emission spectra)

The UV-vis absorption spectra of the complexes were studied (Fig. 3). Reference **Pt-3** gives an absorption band centered at 643 nm, whereas complex **Pt-a** gives absorption at 584 nm (Fig. 3a). The effect of metalation of the π-core of Bodipy on the absorption is clear, that is, with metalation, the absorption of the Bodipy unit is red-shifted as compared with that of the free ligand.[13] For **Pt-1**, the absorption band covers the range 450–700 nm, which is clearly much broader than the complexes with a single visible light-absorbing ligand, such

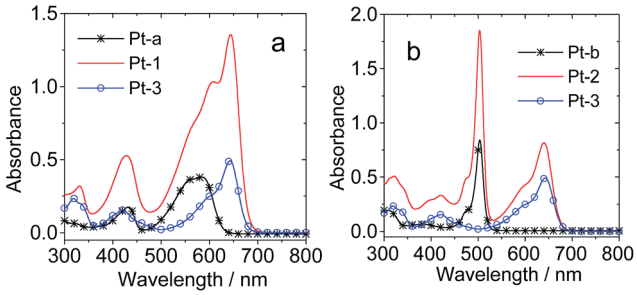

Fig. 3 UV-vis absorption spectra of the complexes. (a) **Pt-a**, **Pt-1** and **Pt-3**. (b) **Pt-b**, **Pt-2** and **Pt-3**. $c = 1.0 \times 10^{-5}$ M in toluene, 20 °C.

as **Pt-a** and **Pt-3**. The absorption band at 643 nm of **Pt-1** is attributed to the central coordinated ligand, as demonstrated by **Pt-3**. The minor absorption bands at 606 nm and 565 nm are attributed to the peripheral Bodipy ligands, as demonstrated by complex **Pt-a**.

No long range π-conjugation exists between the two difference Bodipy units across the Pt(II) centers in **Pt-1**. This postulation is supported by the same absorption band at 643 nm of **Pt-3** as compared with the absorption band at 644 nm for **Pt-1**. This finding is different from the previously reported Pt(II) complexes,[42] for which the absorption of one coordination ligand can be affected by the other coordination ligands in the molecule, demonstrated with the platinum–acetylide copolymers.[43] **Pt-2** shows two well-separated absorption bands at 504 nm and 640 nm (Fig. 3b). By comparison of the shape and energy of the absorption bands with that of the references **Pt-b** and **Pt-3**, the two major absorption bands of **Pt-2** can be assigned to the peripheral 4′-phenyl coordinated Bodipy unit and the central coordinated Bodipy unit, respectively.[43] The absorption of **Pt-2** is the sum of the reference compounds **Pt-3** and **Pt-b** (Fig. 3b).

Therefore we propose that there is no significant electronic interaction between the two different coordination units in **Pt-2**. No $S_0 \rightarrow T_1$ absorption bands were observed for the complexes.[44] We found that the absorption bands of **Pt-1** and **Pt-2** are *not* broader than those of the complexes **Pt-a** and **Pt-b**, thus the numbers of the conformers of **Pt-1** and **Pt-2** in liquid solution are limited otherwise the broadening of the absorption bands should be observed.[45]

The UV-vis absorption maxima on the higher energy side of the absorption spectra of complexes **Pt-1** and **Pt-2** are identical to those of complexes **Pt-a** and **Pt-b**, respectively. Conversely, the absorption maxima on the lower energy side of the spectra are identical to that of complex **Pt-3**. Therefore, the Franck–Condon singlet excited states of the complexes are spatially confined to respective acetylide ligands, and there is no π-conjugation across the Pt(II) atom, otherwise red-shifted absorption bands will be observed for **Pt-1** or **Pt-2**. This finding is different from the previously reported delocalized Franck–Condon singlet excited states in Pt(II) acetylide copolymers containing phenyl and thienyl acetylide ligands.[43,45–47] Previously Pt(II) complexes with a

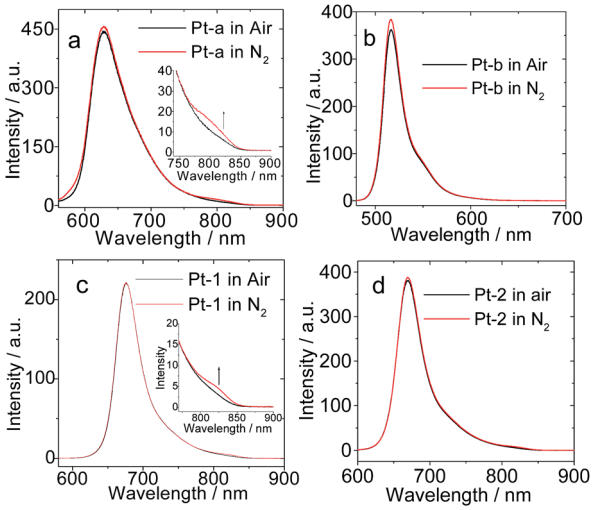

Fig. 4 Emission of the complexes under N_2 and air atmospheres. (a) **Pt-a** ($\lambda_{ex} = 550$ nm), (b) **Pt-b** ($\lambda_{ex} = 470$ nm), (c) **Pt-1** ($\lambda_{ex} = 570$ nm), and (d) **Pt-2** ($\lambda_{ex} = 590$ nm). $c = 1.0 \times 10^{-5}$ M in aerated or deaerated toluene at 20 °C.

Bodipy ligand were reported, but these complexes show '*narrow*' absorption bands in the visible spectral region.[48]

The luminescence spectra of the complexes were studied (Fig. 4). **Pt-a** gives emission at 627 nm. The emission intensity is the same in both aerated and deaerated solutions. The luminescence lifetime of this emission band was determined to be 0.24 ns. These features and the small Stokes shift indicate that the luminescence is fluorescence. A minor emission band at 800 nm was observed and the emission intensity is reduced in aerated solution. Thus this emission band is most likely originated from a triplet emissive state, *i.e.* the emission band at 800 nm is phosphorescence. A similar emission feature was observed for **Pt-1** (Fig. 4c). For complexes **Pt-b** and **Pt-2** (Fig. 4b and d), only fluorescence emission bands were observed. The major emission band of both **Pt-1** and **Pt-2** is at 670 nm. In contrast, the emission of complexes **Pt-a** and **Pt-b** shows blue-shifting of 42 nm and 46 nm, respectively, as compared with that of **Pt-1** and **Pt-2**, probably due to the different coordination profile of the Pt(II) centers.

Pt-1 shows a similar minor emission band at 825 nm, but **Pt-2** does not show such emission. We propose that the emission band of **Pt-1** at 825 nm is due to the peripheral coordination Bodipy ligand. Note that the energy gap between the S_1 and T_1 states of **Pt-1** is 0.26 eV, much smaller than those of the linear Pt(ii) ethynylene complexes with simple organic acetylene ligands (*ca.* 0.7 eV).[42] A small S_1–T_1 state energy gap is beneficial for fast ISC.[42]

In order to study the intramolecular singlet energy transfer, the luminescence of the complexes was compared (Fig. 5: the solutions are with the same optical density at the excitation wavelength). The emission of **Pt-1** is, at 669 nm, different from that of **Pt-a** (Fig. 5a). Similarly, the emission of **Pt-b** at 516 nm was significantly quenched in **Pt-2**. Singlet energy transfer is the

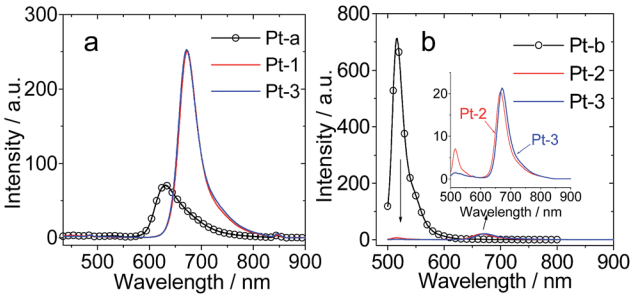

Fig. 5 Emission of the complexes to demonstrate intramolecular singlet energy transfer. (a) **Pt-a** ($c = 2.0 \times 10^{-5}$ M), **Pt-1** ($c = 0.5 \times 10^{-5}$ M) and **Pt-3** ($c = 1.0 \times 10^{-5}$ M), $\lambda_{ex} = 424$ nm. (b) **Pt-b** ($c = 1.0 \times 10^{-5}$ M), **Pt-2** ($c = 0.3 \times 10^{-5}$ M) and **Pt-3** ($c = 1.0 \times 10^{-5}$ M). $\lambda_{ex} = 490$ nm. In (a) or (b), optically matched solutions at the excitation wavelength were used therefore the concentrations are different; in deaerated toluene, 20 °C.

plausible reason for the quenching effect of the emission of **Pt-a** and **Pt-b** in the triads.

To evaluate the intramolecular energy transfer efficiency, the luminescence excitation spectra of the complexes were compared with the UV-vis absorption spectrum (Fig. 6).[27b] Good superimposition between the excitation spectrum and the UV-vis absorption spectrum was observed, indicating an efficient RET effect in **Pt-1**. For **Pt-2**, two well-separated bands in the excitation spectrum were found. With normalization of the band at 640 nm, the excitation band at 502 nm is weaker than the corresponding UV-vis absorption band. The singlet energy transfer in **Pt-2** from the peripheral Bodipy coordinated ligand to the central coordinated Bodipy part was calculated to be 44.8%.[27b] The inefficient intramolecular energy transfer can be attributed to the intramolecular electron transfer or inappropriate dipole moment orientation, the poor spectral overlap, *etc.*[49,50] We noted the discrepancy between the results obtained by quenching studies and the excitation/absorption comparison, which is a lasting question in RET.[27b] The photophysical properties of the complexes are listed in Table 3. **Pt-1**, **Pt-2** and **Pt-a** show weak fluorescence ($\Phi_F < 5\%$), but complex **Pt-b** shows much stronger fluorescence ($\Phi_F = 27.7\%$). The singlet oxygen ($^1O_2$) quantum yields

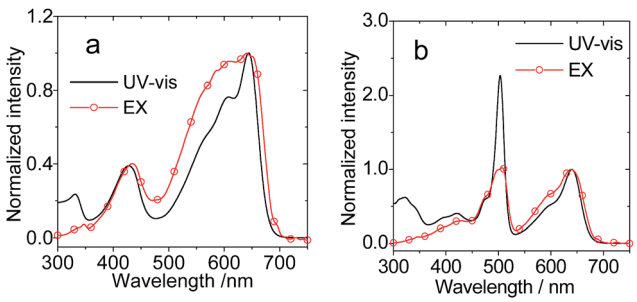

Fig. 6 Comparison of the normalized UV-vis absorption and the luminescence excitation spectra of the complexes. (a) **Pt-1** ($\lambda_{em} = 695$ nm) and (b) **Pt-2** ($\lambda_{em} = 690$ nm). $c = 1.0 \times 10^{-5}$ M in deaerated toluene at 20 °C.

Table 3 Photophysical properties of the ligands and Pt(II) complexes

	λ_{abs}[a]/nm	ε[b]	λ_{em}[a]	Φ_F[c]/%	τ_F[d]/ns	τ_T[e]/μs	Φ_Δ/%
2	505	8.70	519	20.9	2.71	—[f]	—[f]
3	543	11.0	560	—[f]	5.52	—[f]	—[f]
Pt-a	432/584	1.75/3.80	627	0.89	0.24	62.48	69.8%[g]
Pt-b	504	8.427	516	27.7	2.68	607.84	79.3%[h]
Pt-1	428/607/644	5.28/10.3/13.5	669	2.81	0.48	83.87	76.0%[g]
Pt-2	504/640	18.55/8.18	518/662	3.3	—[f]/0.66	100.31	49.7%[g]/78%[h]

[a] In toluene (1.0×10^{-5} M). [b] Molar absorption coefficient, ε: 10^4 M^{-1} cm^{-1}. [c] Fluorescence quantum yields: **B-6** ($\Phi_F = 10.5\%$ in toluene) was used as a standard for **Pt-a**, **Pt-1**, and **Pt-2**. **DCM** ($\Phi_F = 10\%$ in CH_2Cl_2) was used as a standard for **Pt-b**. [d] Luminescence lifetimes, $c = 1.0 \times 10^{-5}$ M in toluene. [e] Triplet state lifetimes, measured by transient absorptions, $c = 5.0 \times 10^{-6}$ M in toluene. [f] Not applicable. [g] Singlet oxygen quantum yields. Methylene blue (**MB**, $\Phi_\Delta = 57\%$ in **DCM**) was used as a standard. The excitation wavelength for **Pt-a** (λ_{ex} = 590 nm), for **Pt-1** (λ_{ex} = 597 nm) and for **Pt-2** (λ_{ex} = 573 nm). [h] Singlet oxygen quantum yields, 2,6-diiodo-Bodipy ($\Phi_\Delta = 83\%$ in **DCM**) was used as a standard. Different excitation wavelengths for **Pt-b** (λ_{ex} = 486 nm) and for **Pt-2** (λ_{ex} = 505 nm) were used.

(Φ_Δ) of the complexes were also measured (Table 3). The high values indicated efficient ISC in these complexes. Furthermore, the Φ_Δ of **Pt-2** is dependent on excitation wavelength, which is an indication of non-unity intramolecular electron transfer.

The fluorescence lifetimes of **Pt-1** and **Pt-2** were determined to be 0.48 ns and 0.66 ns, respectively. These values are very close to the fluorescence lifetime of the reference complex **Pt-3** which contains only the central coordinated Bodipy ligand (0.49 ns).[51] Therefore, we propose that there is no significant photoinduced intramolecular electron transfer, otherwise the fluorescence lifetimes will be reduced. This postulation is also supported by the similar *triplet* state lifetimes of **Pt-1** and **Pt-2** as compared to the reference complex **Pt-3** (see the later section).[52]

Nanosecond time-resolved transient difference absorption spectroscopy: localization of the triplet excited state

In an effort to study the triplet excited state of the complexes, nanosecond time-resolved transient difference absorption spectra of the complexes were studied (Fig. 7). For **Pt-a** (Fig. 7a), a bleaching band at 566 nm was observed upon nanosecond pulsed laser excitation. This band is due to the depletion of the ground state of the Bodipy moiety upon photoexcitation. A minor bleaching band at 428 nm was also observed, which can be assigned to the ground state depletion of the same species. Transient absorption bands at 366 nm and 470 nm and a broadband in the region of 600–800 nm were observed. These features indicated that triplet excited state localized on the Bodipy part was populated. The decay curve gives the lifetime of 50.0 μs (at $c = 1.0 \times 10^{-5}$ M, Fig. 7b).

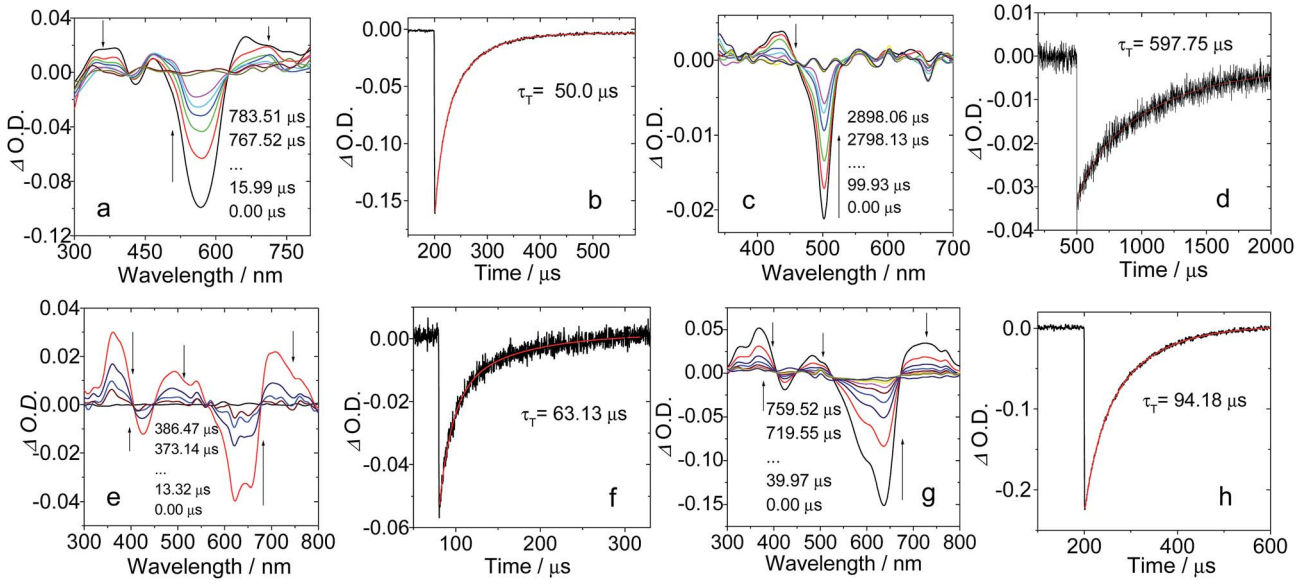

Fig. 7 Nanosecond time-resolved transient difference absorption spectra and the decay curves of the Pt(II) complexes. (a) Complex **Pt-a**, (b) decay of **Pt-a** at 584 nm; (c) **Pt-b**, (d) decay of **Pt-b** at 504 nm (λ_{ex} = 503 nm pulsed laser); (e) **Pt-1**, (f) decay curve of **Pt-1** at 644 nm; (g) **Pt-2**, (h) decay curve of **Pt-2** at 640 nm. With nanosecond pulsed laser excitation (λ_{ex} = 532 nm). $c = 1.0 \times 10^{-5}$ M in deaerated toluene at 20 °C.

For **Pt-b**, a bleaching band at 501 nm was observed (Fig. 7c), where the Bodipy moiety gives strong steady state absorption (Fig. 3b). Thus the triplet excited state of **Pt-b** is localized on the Bodipy ligand, not on the Pt(II) coordination center. The triplet state lifetime is up to 597.75 μs ($c = 1.0 \times 10^{-5}$ M). To the best of our knowledge, this is the *longest* RT triplet excited state lifetime observed for the Bodipy chromophore in transition metal complexes. Previously this value is normally shorter than 100 μs.[30,53–58]

The transient absorption spectra of **Pt-1** show a bleaching band in the region of 550–700 nm (Fig. 7e), which is in agreement with the steady state absorption of **Pt-1**. The bleaching peak at 620 nm is stronger than that at 658 nm. Based on the steady state UV-vis absorption spectrum of **Pt-1**, we propose that the triplet excited state of **Pt-1** is distributed on the three Bodipy ligands, and it is more localized on the peripheral coordinated Bodipy unit, than on the central coordinated Bodipy part. This apparent *delocalization* is most probably due to the degenerated T_1 and T_2 states of the complexes, *i.e.* triplet state equilibrium. This postulation is in agreement with the observation that the 810 nm phosphorescence band of complex **Pt-a** was not quenched in complex **Pt-1**. The triplet state lifetime of 63.13 μs was observed for **Pt-1** (1.0×10^{-5} M). The uniform decay of the two triplet excited states indicated that the two isoenergetic triplet excited states are in fast equilibrium, *i.e.* there is efficient triplet state energy transfer between the different Bodipy ligands in the molecular chain.[41] This conclusion is in agreement with the previous report of triplet excited state energy transfer across the central coordination Pt(II) center.[43] To the best of our knowledge, this is the first time that the excited state equilibrium was observed for the linear Pt(II) arylacetylide complexes.[43] Previously, the T_1 triplet excited state of the Pt(II) acetylide polymer or oligomers was reported to be spatially confined to one ligand.[15] Although triplet state equilibrium was proposed previously, no direct spectral evidence was observed due to other competitive processes such as electron transfer (charge separation).[52]

The transient absorption of **Pt-2** shows a major absorption band at 635 nm (Fig. 7g). Interestingly, no bleaching band at 501 nm was observed. Therefore, the triplet state of **Pt-2** is exclusively confined to the central coordinated Bodipy ligand, not on the peripheral coordinated Bodipy ligand.[43] Since we have shown with **Pt-b** that the triplet state of the peripheral coordinated Bodipy part can be produced upon pulsed laser excitation at 503 nm (Fig. 7c), the lack of the bleaching band at 500 nm of **Pt-2** with pulsed laser excitation at 503 nm (see ESI, Fig. S18†) indicated intramolecular triplet–triplet-energy-transfer (TTET) from the peripheral Bodipy moiety to central Bodipy in **Pt-2**. No triplet state equilibrium was established in **Pt-2** because of the large energy gap between the triplet states localized on the central and the peripheral Bodipy moieties. The triplet state energy level of the unsubstituted Bodipy was determined to be 1.70 eV by phosphorescence,[53] whereas the central coordinated Bodipy moiety is with the triplet state energy level of 1.61 eV.[30] The triplet state lifetime of **Pt-2** was determined to be 94.18 μs ($c = 1.0 \times 10^{-5}$ M^{-1}). The T_1 state lifetime is very long, even with the Pt(II) center π-conjugatedly linked to the Bodipy chromophores,[59] compared to platinum–phenyl acetylide oligomers (normally <25 μs).[45] The observation of the long-lived triplet state with the complexes is unusual considering the low energy level of the coordinated Bodipy ligand (*ca.* 1.6 eV). Usually the triplet state lifetime will be short because the non-radiative decay will be significant with smaller T_1–S_0 energy gap.[60] These long-living T_1 states of the complexes are beneficial for the application of these complexes as the triplet state energy donor to initiate the cascade photophysical processes.[59]

Linear Pt(II) acetylide complexes showing a long-lived T_1 state were rarely reported.[17] Previously Pt(II) acetylide complexes with fluorenyl ligands were reported to show the T_1 state lifetime up to 178–220 μs, but those complexes show weak absorption of visible light.[47] Notably the long-living triplet state of **Pt-1** and **Pt-2** is not compromised by any low triplet state yield indicated by the high singlet oxygen ($^1O_2$) quantum yields (Φ_Δ, Table 3).[44] A similar triplet state lifetime of the complexes **Pt-1**, **Pt-2**, and **Pt-a** and the reference complex **Pt-3** (64.3 μs)[51] indicated that there is no significant photoinduced intramolecular electron transfer for **Pt-1** and **Pt-2**, otherwise the triplet state lifetimes will be substantially reduced.[52] Furthermore, all the transient absorption features ($T_1 \rightarrow T_n$ transitions) are similar to that observed for the Pt(II) Bodipy acetylide complex, thus the compelling evidence shows that the transient species are due to the triplet excited state of the coordinated Bodipy ligands, not charge separated states.[52]

Calculation of the free energy changes of the photoinduced intramolecular electron transfer

The study of the triplet excited state implies that no significant electron transfer exists for complexes **Pt-1** and **Pt-2**, because the triplet state lifetimes of **Pt-1** and **Pt-2** are close to those of complexes **Pt-a** and **Pt-3**. This conclusion was supported by calculation of the free energy changes (ΔG°_{CS}) of the photoinduced intramolecular electron transfer with the Weller equation.

First, we assume that the triplet excited state of **Pt-1** and **Pt-2** is responsible to initiate the photo-induced intramolecular electron transfer. Based on the electrochemical properties of the complexes (Table 2), the central coordinated Bodipy moiety was considered as the electron donor ($E^{OX}_{1/2} = +0.43$ V), and the peripheral coordinated Bodipy as the electron acceptor ($E^{RED}_{1/2} = -1.56$ V). The $E_{0,0}$ value was approximated by the phosphorescence of **Pt-1** (*ca.* 1.55 eV). Therefore the free energy change of electron transfer of **Pt-1** was approximated as $\Delta G^\circ_{CS} = e[E_{OX} - E_{RED}] - E_{0,0} = 0.43 - (-1.56) - 1.55 = +0.44$ eV (the static Columbic energy is usually small and was not considered here). Thus, the triplet excited state of **Pt-1** is unlikely to drive intramolecular electron transfer. Similarly a positive value of +0.45 eV was determined for **Pt-2**. If the singlet excited state of **Pt-1** and **Pt-2** was responsible to drive intramolecular electron transfer ($E_{0,0}$ is approximated with the fluorescence emission wavelength as *ca.* 1.85 eV), $\Delta G^\circ_{CS} = +0.14$ eV and $\Delta G^\circ_{CS} = +0.15$ eV were obtained for **Pt-1** and **Pt-2**, respectively. Thus, no photoinduced electron transfer is expected for **Pt-1** and **Pt-2**.

Femtosecond time-resolved transient difference absorption spectroscopy: singlet energy transfer

The two kinds of Bodipy ligand in **Pt-2** show substantially different absorption wavelengths (Fig. 3b), thus **Pt-2** is ideal for the study of the ultrafast singlet energy transfer. Femtosecond ultrafast pump–probe experiments were performed for **Pt-2** at 504 nm and 640 nm pump wavelength to excite the singlet state of the peripheral BODIPY part and central coordinated BODIPY part, respectively ($S_0 \rightarrow S_1$) (Fig. 8). Upon excitation of **Pt-2** at 504 nm, bleaching bands were observed around 505 nm and 650 nm where the peripheral BODIPY part and central coordinated BODIPY part give the steady state absorption, respectively. While the bleaching signal around 505 nm decreases, the bleaching signal around 650 nm increases concomitantly (Fig. 8). The decay time of the bleaching signal of the peripheral Bodipy part (around 505 nm) is about 25 ps, which is approximately equal to the rise time of the bleaching signal of the central coordinated Bodipy part (around 650 nm, Fig. 8b). This process indicates singlet energy transfer from the peripheral Bodipy part to central coordinated Bodipy part ($k_{EnT} = 4.0 \times 10^{10}$ s^{-1}). On the other hand, a positive signal (excited state absorption) appears above 680 nm probe wavelength after 800 ps delay time (independent of the pump wavelength). This signal can be attributed to the T_1–T_n transition.

In addition, an extra pump probe experiment was performed with 640 nm pump wavelength (see ESI, Fig. S19†). There is a single bleaching signal at 650 nm, which corresponds to the singlet state of the central coordinated BODIPY part and no singlet energy transfer is expected. Furthermore, a similar T_1–T_n transition was observed as a positive signal at the same wavelength (680 nm).

DFT calculations on the photophysical properties of the complexes

The spin density surfaces of the complexes were calculated (Fig. 9). For **Pt-a** and **Pt-b**, the spin density is localized on the Bodipy unit, not on the Pt(II) coordination centre. This result is in agreement with the transient absorption spectra (Fig. 7). For **Pt-1**, the spin density surface is localized on the peripheral coordinated Bodipy part. Since the spin density surface shows the location of only the T_1 state, this result is in agreement with the nanosecond time-resolved transient difference absorption, which indicates that the triplet state is more localized on the peripheral Bodipy moiety (Fig. 7), as well as the fact that the phosphorescence of the peripheral coordinated Bodipy (**Pt-a**) is retained in **Pt-1** (Fig. 4).

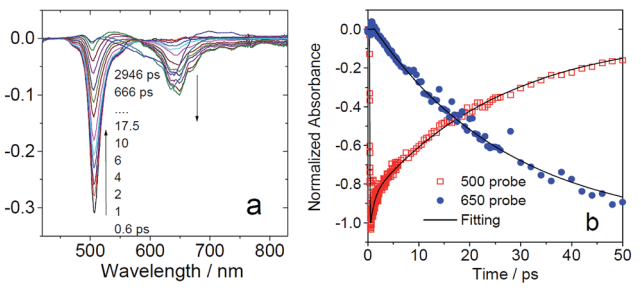

Fig. 8 Picosecond ultrafast transient absorption spectra of **Pt-2** upon femtosecond pulsed laser excitation at 504 nm. (a) Transient absorption spectra after pulsed laser excitation at 504 nm. (b) Decay traces at 500 nm and 650 nm. $c = 1.0 \times 10^{-5}$ M in toluene at 20 °C.

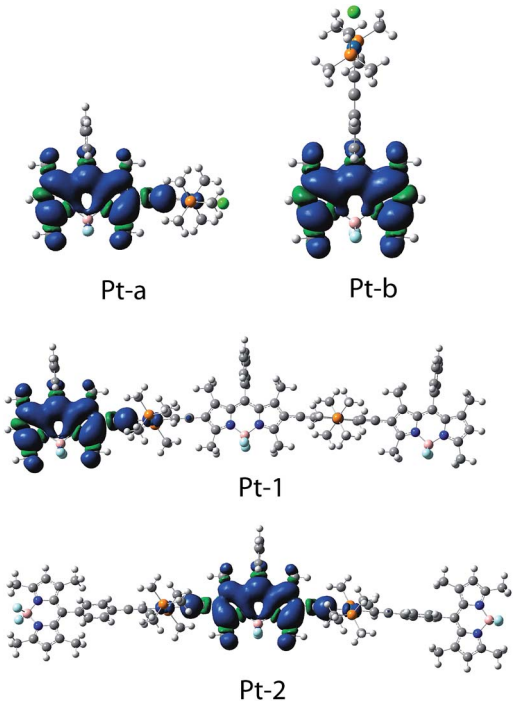

Fig. 9 Isosurfaces of spin density of the complexes **Pt-a**, **Pt-b**, **Pt-1** and **Pt-2**. Calculated at the optimized triplet state geometries. Toluene was used as a solvent in the calculations (PCM model). Calculation was performed at the B3LYP/GENECP/LANL2DZ level with Gaussian 09W.

For **Pt-2**, the spin density is exclusively localized on the central coordinated Bodipy ligand, and the peripheral coordinated Bodipy ligand does not contribute to the spin density surface at all. This finding is in full agreement with the transient absorption spectrum (Fig. 7g). Based on the spin density surface, the T_1 state of **Pt-2** is highly confined to the central Bodipy ligand (Fig. 9).[46]

For **Pt-1** and **Pt-2**, the common feature of the spin density surface is the minor contribution of the Pt(II) atom. With the large π-conjugation ligand, the S_1 and T_1 states are more localized on the ligand, therefore the $^3IL \rightarrow S_0$ transition is assumed to be a strongly forbidden transition, which may be responsible for the long lifetime of the T_1 state of the complexes.[44]

The electronic structures of the singlet excited states and the triplet excited states of the complexes **Pt-1** and **Pt-2** were studied in detail by DFT and TDDFT methods. HOMO → LUMO+1 is involved in the $S_0 \rightarrow S_1$ transition of **Pt-1** (Fig. 10), thus the S_1 state is featured with a charge transfer character. The S_3 state is localized on the central coordinated Bodipy unit. The S_{18} state is mainly localized on the peripheral Bodipy ligands.

The triplet state of **Pt-1** was studied by the TDDFT method based on the ground state geometry (Table 4). HOMO →

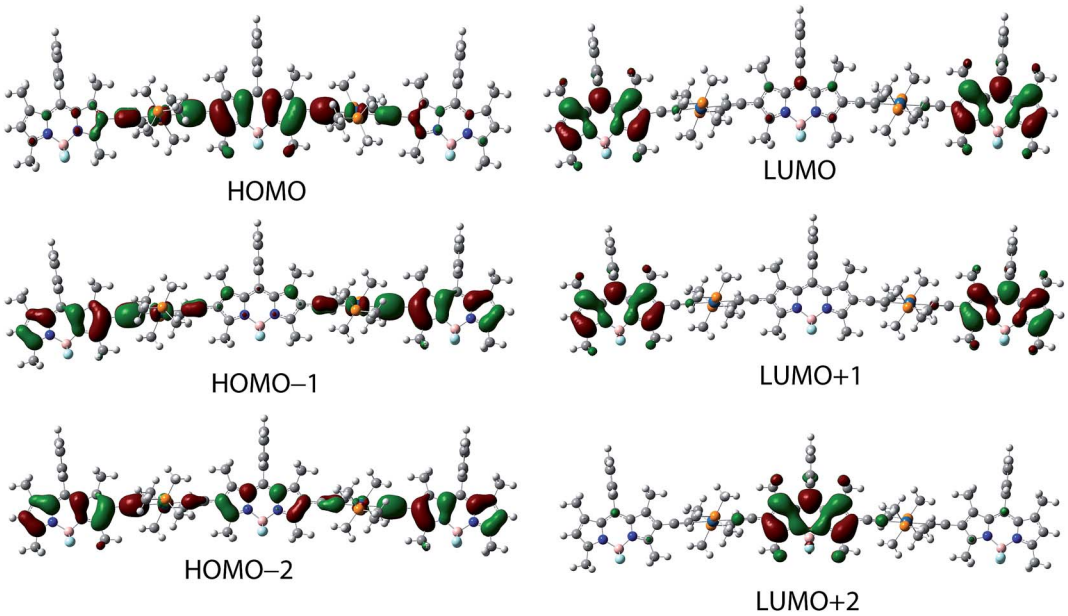

Fig. 10 Electron density maps of the frontier molecular orbitals of complex **Pt-1** based on the optimized ground state geometry. The solvent toluene was considered in the calculations (PCM model). Calculated at the B3LYP/GENCP/LANL2DZ level with Gaussian 09W.

LUMO+2 is involved in the T_1 state, thus the T_1 state is localized on the central coordinated Bodipy unit to a large extent. HOMO−1 and LUMO+1 are involved in the T_2 state. Thus the T_2 state is localized on the peripheral Bodipy unit.

The electronic structure of the singlet excited state and the triplet excited state of **B-2** was also studied by the DFT and the TDDFT calculations (Fig. 11 and Table 5). The $S_0 \rightarrow S_1$ transition is composed of HOMO → LUMO, both orbitals are localized on the central coordination Bodipy unit. We found degenerated S_2 and S_3 states (Table 5), for which HOMO−3 → LUMO+1 and HOMO−2 → LUMO+1 are involved, respectively. S_2 and S_3 states are localized on the peripheral coordinated Bodipy units (Fig. 11). We noted the discrepancy between the calculated excitation energy (UV-vis absorption) and the experimental values. This result is within expectation because it is known that the DFT theory usually overestimated the excitation energy of Bodipy compounds.[61]

The triplet states of **Pt-2** were studied by similar methods based on the ground state geometry (Fig. 11 and Table 5). HOMO and LUMO are involved in the T_1 state (Table 5). Thus it is clear that the T_1 state is localized on the central coordinated Bodipy unit. This conclusion is in agreement with the nanosecond time-resolved transient difference absorption spectra of **Pt-2** (Fig. 7). Degenerated T_2 and T_3 states were observed for **Pt-2** (energy level is 1.39 eV). Inspection of the MOs involved in T_2 and T_3 states indicates that these triplet states are localized on the peripheral coordinated Bodipy units.

The photophysical process of **Pt-1** and **Pt-2** are summarized in Scheme 3. For **Pt-1**, the UV-vis absorption spectrum indicated that the peripheral coordinated Bodipy part shows higher

Table 4 Excitation energies (eV) and corresponding oscillator strengths (f), main configurations and CI coefficients of the low-lying electronically excited states of **Pt-1**, calculated by TDDFT//B3LYP/LANL2DZ, based on the DFT//B3LYP/LANL2DZ optimized ground state geometries

	TDDFT/B3LYP/LANL2DZ					
	Electronic transition	Energy[a] [eV / nm]	f[b]	Composition[c]	CI[d]	Character
Singlet	$S_0 \rightarrow S_1$	1.98/626	0.4889	H → L+1	0.6277	MLCT/ILCT
	$S_0 \rightarrow S_2$	2.00/617	0.1335	H → L	0.6462	MLCT/ILCT
	$S_0 \rightarrow S_3$	2.12/585	0.7147	H → L+2	0.6651	MLCT
	$S_0 \rightarrow S_4$	2.18/568	0.0823	H−1 → L+1	0.6115	MLCT
	$S_0 \rightarrow S_{18}$	2.87/432	0.7453	H−6 → L+1	0.5981	MLCT/ILCT
	$S_0 \rightarrow S_{23}$	3.10/400	0.5790	H−8 → L+2	0.5041	ILCT
Triplet	$S_0 \rightarrow T_1$	1.35/919	0.0000[e]	H → L+2	0.6168	MLCT
	$S_0 \rightarrow T_2$	1.40/884	0.0000[e]	H−1 → L+1	0.5452	MLCT
	$S_0 \rightarrow T_3$	1.43/868	0.0000[e]	H−2 → L	0.5379	MLCT/ILCT

[a] Only the selected low-lying excited states are presented. [b] Oscillator strengths. [c] Only the main configurations are presented. [d] The CI coefficients are in absolute values. [e] No spin–orbital coupling effect was considered, thus the f values are zero.

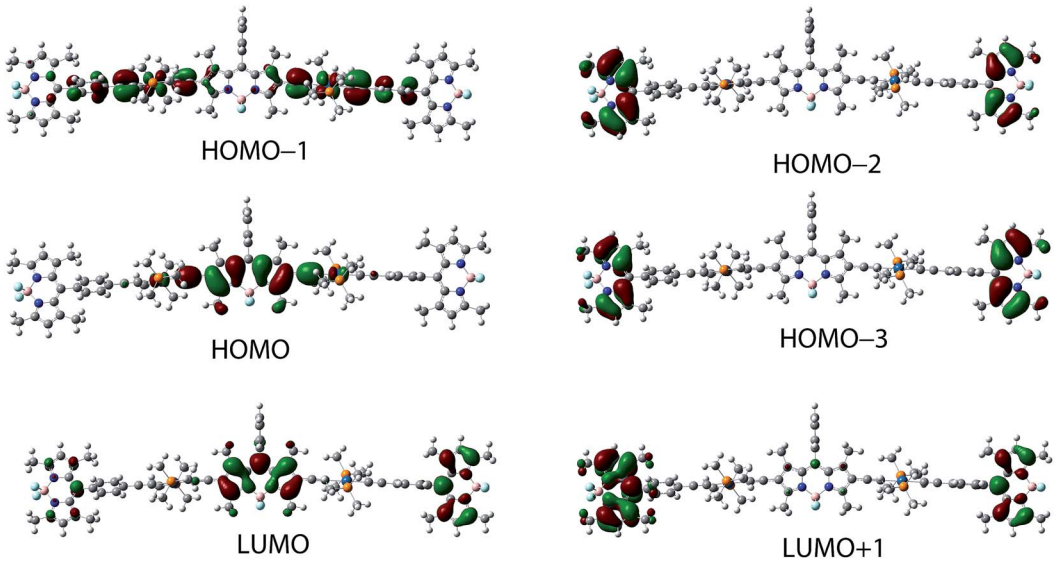

Fig. 11 Electron density maps of the frontier molecular orbitals of **Pt-2** based on the optimized ground state geometry. The solvent toluene was considered in the calculations (PCM model). Calculated at the CAM-B3LYP/SDD/LANL2DZ level with Gaussian 09W.

singlet state energy (^{1}[BDP*-p] in Scheme 3) than the central coordinated Bodipy part (^{1}[BDP*-c] in Scheme 3). The luminescence emission studies show that the fluorescence of the ^{1}[BDP*-p] part was quenched in **Pt-1**, *i.e.* the singlet excited state of the peripheral coordinated Bodipy is with a slightly higher energy level than the central coordinated Bodipy moiety does, thus the singlet energy transfer from the ^{1}[BDP*-p] to ^{1}[BDP*-c] takes place. As a result, only the fluorescence emission from the ^{1}[BDP*-c] part can be observed. Both coordination parts can undergo ISC to give the triplet excited state. The two triplet excited states localized on the central and the peripheral Bodipy parts are in fast equilibrium, since the two triplet excited states decay uniformly (Fig. 7e). Triplet excited state equilibrium in transition metal complexes was rarely reported.[62]

For **Pt-2**, the difference between the S_1 state energy levels of the peripheral and the central Bodipy parts is more distinct than that of **Pt-1**. Based on the transient absorption spectra, no triplet state equilibrium was observed for **Pt-2**. Thus we propose that the ^{3}[BDP*-p] state was quenched by the efficient triplet state energy transfer to ^{3}[BDP*-c]. This photophysical process is different from that of **Pt-1**.

Triplet–triplet annihilation upconversion with the complexes as triplet photosensitizers

The complexes show strong absorption of visible light and long-lived triplet excited states, thus these complexes can be used as triplet photosensitizers for TTA upconversion.[13,63] Among the upconversion methods, TTA upconversion is of particular interest, due to its strong absorption of visible light, high upconversion quantum yields, and tunable excitation/emission wavelength. Non-coherent, low power excitation light is sufficient for this kind of upconversion, such as solar light.[64–68] Conventional triplet photosensitizers for TTA upconversion are

Table 5 Excitation energies (eV) and corresponding oscillator strengths (f), main configurations and CI coefficients of the low-lying electronically excited states of complex **Pt-2**. Calculated by TDDFT//B3LYP/LANL2DZ, based on the DFT//B3LYP/LANL2DZ optimized ground state geometries

	TDDFT/CAM-B3LYP/SDD					
	Electronic transition	Energy[a] [eV / nm]	f[b]	Composition[c]	CI[d]	Character
Singlet	$S_0 \rightarrow S_1$	2.49/497	1.1904	H → L	0.5334	MLCT
	$S_0 \rightarrow S_2$	2.90/426	0.0665	H−3 → L+1	0.4587	
	$S_0 \rightarrow S_3$	2.91/426	1.3281	H−2 → L+1	0.4759	ILCT
	$S_0 \rightarrow S_4$	3.34/370	0.1169	H−5 → L	0.4774	MLCT
	$S_0 \rightarrow S_5$	3.48/356	0.4370	H−6 → L	0.5125	MLCT
Triplet	$S_0 \rightarrow T_1$	1.30/951	0.0000[e]	H → L	0.4904	MLCT
	$S_0 \rightarrow T_2$	1.39/891	0.0000[e]	H−2 → L+1	0.4554	ILCT
	$S_0 \rightarrow T_3$	1.39/891	0.0000[e]	H−3 → L+1	0.3462	

[a] Only the selected low-lying excited states are presented. [b] Oscillator strengths. [c] Only the main configurations are presented. [d] The CI coefficients are in absolute values. [e] No spin–orbital coupling effect was considered, thus the f values are zero.

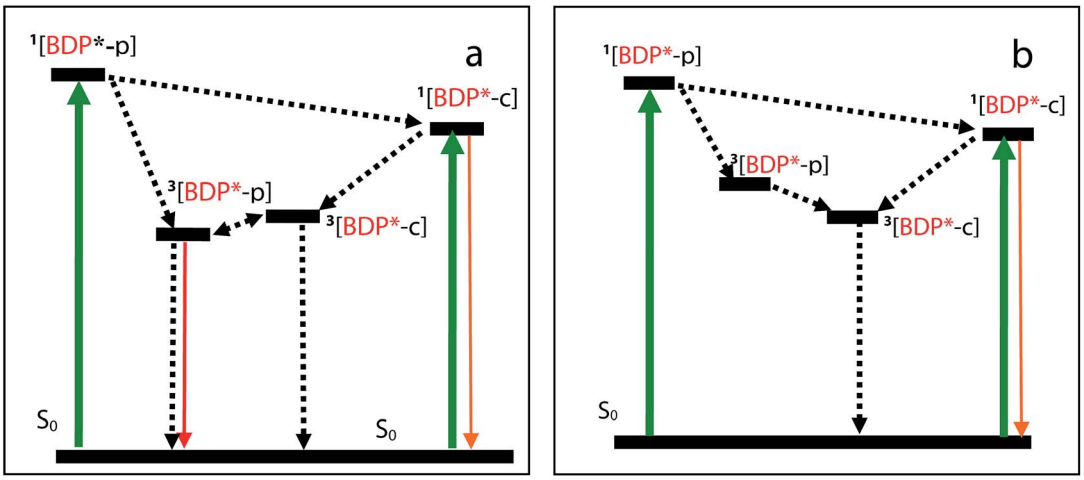

Scheme 3 Qualitative energy level diagram of complexes (a) **Pt-1** and (b) **Pt-2**. BDP stands for Bodipy. BDP-c stands for the central coordination Bodipy part. BDP-p stands for the peripheral coordination Bodipy part.

limited to Pt(II) or Pd(II) porphyrin complexes.[64,65,69,70] Recently we developed a series of Ru(II), Pt(II), Ir(III) and Re(I) complexes for TTA upconversion; all these complexes show strong absorption of visible light and long-lived triplet excited states.[13,65] However, to the best of our knowledge, no complexes showing *broadband* visible light absorption have been used as a triplet photosensitizer for TTA upconversion. It will become possible to carry out multi-wavelength excitable upconversion with the complexes **Pt-1** and **Pt-2**, which may be suitable for TTA upconversion with a broadband excitation source.

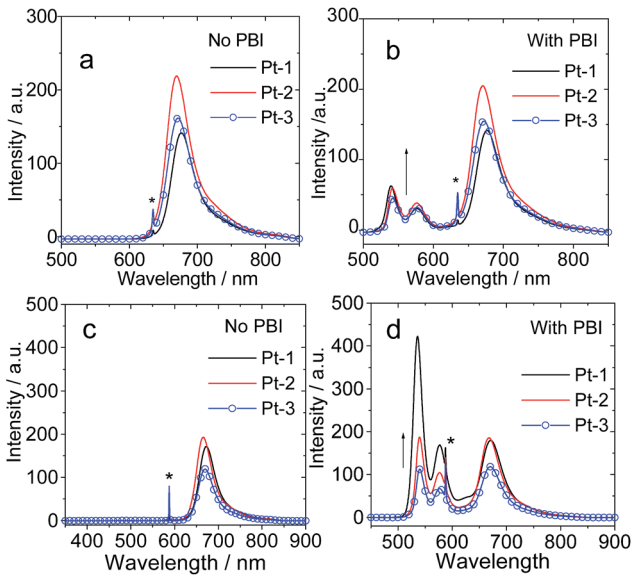

Fig. 12 Upconversion with **Pt-1**, **Pt-2** and **Pt-3** as the triplet photosensitizers and **PBI** as a triplet acceptor. (a) Photoluminescence spectra of the photosensitizers alone at 635 nm excitation (10 mW). (b) Photoluminescence spectra in the presence of **PBI**. Excited with a 635 nm laser (10 mW). (c) Photoluminescence spectra of the photosensitizers alone at 589 nm excitation (5 mW). (d) Photoluminescence spectra of the complexes in the presence of **PBI**. Excited with a 589 nm laser (5 mW). For **Pt-1**, c [**PBI**] = 2.6×10^{-5} M; for **Pt-2**, c [**PBI**] = 4.0×10^{-5} M; for **Pt-3**, c [**PBI**] = 4.1×10^{-5} M. The asterisks indicate the scattered laser (589 nm and 635 nm). c [photosensitizers] = 1.0×10^{-5} M in deaerated toluene at 20 °C.

First a 635 nm laser was used for excitation. All the complexes **Pt-1**–**Pt-3** give strong fluorescence at 670 nm (Fig. 12a). In the presence of a triplet energy acceptor **PBI**, emission bands in the region of 510–600 nm were observed (Fig. 12b). Excitation of **PBI** alone with a 635 nm laser did not produce any emission bands in the same region. Thus, these new emission bands can be attributed to the upconverted emission of **PBI**. Upconversion quantum yields of 1.53%, 1.19% and 2.42% were determined for **Pt-1**–**Pt-3**, respectively.

Since these complexes show broadband absorption in the region of 500–700 nm, we also used another excitation wavelength (589 nm) for the TTA upconversion (Fig. 12c and d). Interestingly, we found that the TTA upconversion is stronger as compared with that excited at 635 nm. For example, the upconverted emission intensity in the region of 500–600 nm is stronger than the residual fluorescence of the complexes, which can be treated as an internal standard. The upconversion quantum yields were determined to be 9.72%, 4.89% and 9.84% for **Pt-1**–**Pt-3**, respectively with excitation at 589 nm.

The upconversion can be performed in dim light, for example, the light from a spectrofluorometer (see ESI, Fig. S20†). TTA upconversion was observed with **Pt-1** and **Pt-2** by excitation at 600–620 nm with a spectrofluorometer. Other upconversion methods failed to be carried out with weak light as an excitation source.[71]

The TTA upconversion with the complexes as triplet photosensitizers is visible to the naked eye (Fig. 13). For the complexes alone, deep red emission was observed upon 635 nm laser excitation. In the presence of a triplet acceptor/emitter **PBI**, strong green emission was observed. Such strong and unaided eye-visible upconversion will be promising for applications in luminescence bioimaging[72–75] or solar cells.[76–78]

The delayed fluorescence of the TTA upconversion was studied (Fig. 14). Firstly, we studied the fluorescence emission of **Pt-1** alone. Interestingly, we observed long-lived luminescence

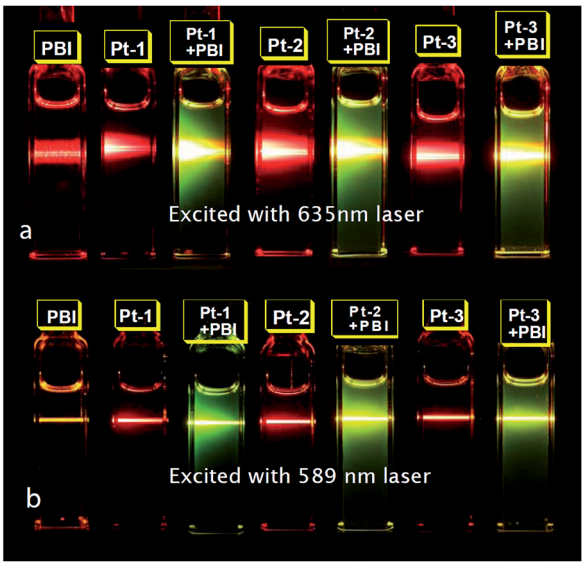

Fig. 13 Photographs of the TTA upconversion. Emission of triplet photosensitizers alone and the TTA upconversion. Excited with a continuous 635 nm laser (10 mW). c [complexes] $= 1.0 \times 10^{-5}$ M. For **Pt-1**, c [**PBI**] $= 2.6 \times 10^{-5}$ M; for **Pt-2**, c [**PBI**] $= 4.0 \times 10^{-5}$ M in deaerated toluene at 20 °C.

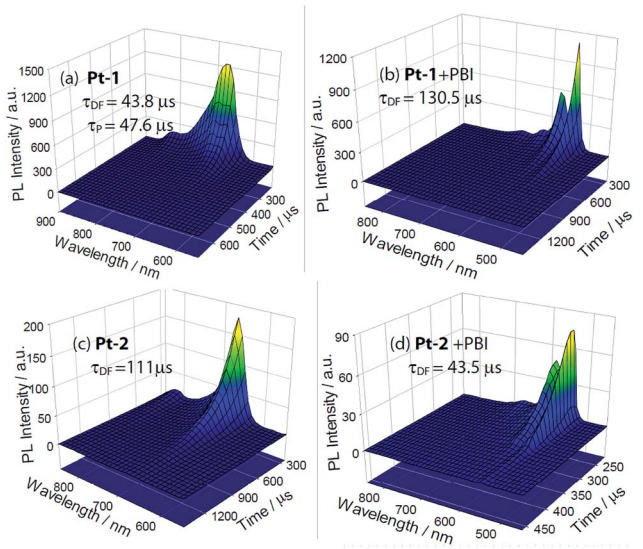

Fig. 14 Time-resolved emission spectra (TRES) of **Pt-1**, **Pt-2** alone and the TTA upconversion with **PBI** as a triplet acceptor. (a) **Pt-1** alone, the fluorescence and phosphorescence regions were measured (550–850 nm, $\tau_{DF} = 43.8$ ms, $\tau_P = 47.6$ ms). (b) TRES of **Pt-1** in the presence of **PBI**. Upconverted emission in the range of 500–600 nm was observed ($\tau_{DF} = 130.5$ μs). (c) TRES of **Pt-2** alone. The fluorescence region was measured (550–850 nm, $\tau_{DF} = 111.0$ μs). (d) TRES of **Pt-2** in the presence of **PBI**. Upconverted emission in the range of 500–600 nm was observed ($\tau = 43.5$ μs). For **Pt-1**, c [**PBI**] $= 4.0 \times 10^{-5}$ M, for **Pt-2**, c [**PBI**] $= 4.0 \times 10^{-5}$ M. c [sensitizers] $= 1.0 \times 10^{-5}$ M in deaerated toluene. Excited with a nanosecond pulsed OPO laser synchronized with a spectrofluorometer ($\lambda_{ex} = 560$ nm), 25 °C.

($\tau_{DF} = 43.8$ μs). The emission features, such as the wavelength and the band shape, are superimposable to the steady state luminescence spectrum of **Pt-1**. The emission of **Pt-1** was also studied in aerated solution, and no signal was observed. Considering that the power of a nanosecond pulsed OPO laser is high, and the long-lived triplet state of **Pt-1**, we propose that the long-lived luminescence is due to the delayed fluorescence, *via* the TTA mechanism. This postulation was supported by the fact that no such long-lived fluorescence can be observed with the picosecond pulsed laser, for which the laser power is much lower. Thus, another mechanism for the delayed fluorescence, *i.e.* the thermally activated reverse ISC, is not responsible for the delayed luminescence of **Pt-1**.[79,80]

Similar delayed luminescence was observed for **Pt-2** ($\tau_{DF} =$ 111.0 μs, in aerated solution, no signal was detected). Delayed luminescence was observed for **Pt-a** (13.7 μs) and **Pt-b** (189.2 μs). The delayed fluorescence of the complexes is due to the long-lived triplet excited states. To the best of our knowledge, the delayed fluorescence of Pt(II) complexes is rarely reported.[17,81–84] Previously it was observed for **Pt-3**.[51] Delayed fluorescence may find applications in time-gated luminescence bioimaging.[85]

In the presence of triplet energy acceptor **PBI**, fluorescence emission in the region of 500–600 nm was observed (Fig. 14b and d), which is the featured fluorescence of **PBI**. The luminescence lifetime was determined to be 130.5 μs and 43.5 μs with **Pt-1** and **Pt-2** as the triplet photosensitizers, respectively. Thus the TTA upconversion was confirmed by the delayed fluorescence of **PBI**.[69]

Conclusions

In summary, two heteroleptic *trans*-bis(alkylphosphine) platinum(II)-alkynyl complexes with three Bodipy ligands were prepared to achieve the goal of broadband absorption of visible light (**Pt-1** and **Pt-2**). Sequential intramolecular resonance energy transfer (RET) and intersystem crossing (ISC) were concerted to transform the harvested broadband photoexcitation energy to triplet excited state energy. Both the singlet energy donor and the acceptor give strong visible light absorption, but at different wavelengths. The singlet energy acceptor is also a spin converter to produce triplet excited states. Two reference complexes with only one visible light-absorbing Bodipy ligand in the molecule were prepared for comparison. Singlet energy transfer from the peripheral coordination Bodipy moiety to the central coordinated Bodipy (with 2,6-diacetyl profile) moiety was confirmed by steady state luminescence spectroscopy, fluorescence excitation spectroscopy and femtosecond ultrafast transient difference absorption spectroscopy. Nanosecond time-resolved transient difference absorption spectroscopy indicated that the triplet excited state of **Pt-1** is *delocalized* on both the peripheral and the central coordinated Bodipy units. For **Pt-2**, however, the T_1 state is confined to the central coordinated Bodipy segment. Long-lived triplet excited states were observed for both complexes ($\tau_T = 63.13$ μs for **Pt-1** and $\tau_T = 94.18$ μs for **Pt-2** at 1.0×10^{-5} M). With pulsed laser excitation, delayed fluorescence was observed for the complexes ($\tau_{DF} = 43.8$ μs for **Pt-1**, $\tau_{DF} = 111.0$ μs for **Pt-2**), which is rarely reported for transition metal complexes. The complexes were used for multi-

wavelength excitable triplet–triplet annihilation upconversion. Furthermore, the efficient singlet and triplet energy transfer for the chromophores across the center coordinating Pt(II) center will be fundamentally important for investigation of the photochemistry of Pt(II) complexes and for construction of functional molecular arrays with these photoresponsive units. Our results are useful for preparation of transition metal complexes that show broadband absorption of visible light and long-lived triplet excited states, for the study of the fundamental photochemical properties of transition metal complexes and the applications in photocatalysis, luminescence bioimaging photodynamic therapy and upconversion.

Acknowledgements

We thank the NSFC (21073028, 21273028, 21421005 and 21473020), the Royal Society (UK) (China–UK Cost-Share Science Networks), the Ministry of Education (SRFDP-20120041130005), the Program for Changjiang Scholars and Innovative Research Team in University [IRT_13R06], the State Key Laboratory of Fine Chemicals (KF1203), the Fundamental Research Funds for the Central Universities (DUT14ZD226) and Dalian University of Technology (DUT2013TB07) for financial support.

References

1 (*a*) I. Eryazici, C. N. Moorefield and G. R. Newkome, *Chem. Rev.*, 2008, **108**, 1834–1895; (*b*) E. E. Langdon-Jones and S. J. A. Pope, *Chem. Commun.*, 2014, **50**, 10343–10354.
2 K. A. Nguyen, P. N. Day and R. Pachter, *J. Phys. Chem. A*, 2009, **113**, 13943–13952.
3 R. Liu, D. Zhou, A. Azenkeng, Z. Li, Y. Li, K. D. Glusac and W. Sun, *Chem.–Eur. J.*, 2012, **18**, 11440–11448.
4 R. Liu, A. Azenkeng, D. Zhou, Y. Li, K. D. Glusac and W. Sun, *J. Phys. Chem. A*, 2013, **117**, 1907–1917.
5 W. Y. Wong and P. D. Harvey, *Macromol. Rapid Commun.*, 2010, **31**, 671–713.
6 W. Lu, B. X. Mi, M. C. W. Chan, Z. Hui, C. M. Che, N. Zhu and S. T. J. Lee, *J. Am. Chem. Soc.*, 2004, **126**, 4958–4971.
7 K. Y. Kim, S. Liu, M. E. Köse and K. S. Schanze, *Inorg. Chem.*, 2006, **45**, 2509–2519.
8 A. M. Soliman, M. Abdelhameed, E. Z. Colman and P. D. Harvey, *Chem. Commun.*, 2013, **49**, 5544–5546.
9 M. Hissler, A. Harriman, A. Khatyr and R. Ziessel, *Chem.–Eur. J.*, 1999, **5**, 3366–3381.
10 P. Shao, Y. Li, J. Yi, T. M. Pritchett and W. Sun, *Inorg. Chem.*, 2010, **49**, 4507–4517.
11 C. K. M. Chan, C. H. Tao, H. L. Tam, N. Zhu, V. W. W. Yam and K. W. Cheah, *Inorg. Chem.*, 2009, **48**, 2855–2864.
12 H. Guo, S. Ji, W. Wu, W. Wu, J. Shao and J. Zhao, *Analyst*, 2010, **135**, 2832–2840.
13 (*a*) J. Zhao, S. Ji, W. Wu, W. Wu, H. Guo, J. Sun, H. Sun, Y. Liu, Q. Li and L. Huang, *RSC Adv.*, 2012, **2**, 1712–1728; (*b*) J. Zhao, W. Wu, J. Sun and S. Guo, *Chem. Soc. Rev.*, 2013, **42**, 5323–5351.
14 E. O. Danilov, I. E. Pomestchenko, S. Kinayyigit, P. L. Gentili, M. Hissler, R. Ziessel and F. N. Castellano, *J. Phys. Chem. A*, 2005, **109**, 2465–2471.
15 K. Glusac, M. E. Köse, H. Jiang and K. S. Schanze, *J. Phys. Chem. B*, 2007, **111**, 929–940.
16 T. Kindahl, P. G. Ellingsen, C. Lopes, C. Brannlund, M. Lindgren and B. Eliasson, *J. Phys. Chem. A*, 2012, **116**, 11519–11530.
17 J. A. G. Williams, *Top. Curr. Chem.*, 2007, **281**, 205–268.
18 (*a*) S. C. F. Kui, S. S.-Y. Chui, C.-M. Che and N. Zhu, *J. Am. Chem. Soc.*, 2006, **128**, 8297–8309; (*b*) W. Y. Wong and C. L. Ho, *Coord. Chem. Rev.*, 2006, **250**, 2627–2690.
19 L. Liu, S. Guo, J. Ma, K. Xu, J. Zhao and T. Zhang, *Chem.–Eur. J.*, 2014, DOI: 10.1002/chem.201403780, accepted.
20 K. Y. Kim, A. H. Shelton, M. Drobizhev, N. Makarov, A. Rebane and K. S. Schanze, *J. Phys. Chem. A*, 2010, **114**, 7003–7013.
21 J. Chen, G. Zhao, T. R. Cook, X. Sun, S. Yang, M. Zhang, K. Han and P. J. Stang, *J. Phys. Chem. A*, 2012, **116**, 9911–9918.
22 C. K. M. Chan, C. Tao, K. Li, K. M. C. Wong, N. Zhu, K. W. Cheah and V. W. W. Yam, *Dalton Trans.*, 2011, **40**, 10670–10685.
23 J. E. Rogers, J. E. Slagle, D. M. Krein, A. R. Burke, B. C. Hall, A. Fratini, D. G. McLean, P. A. Fleitz, T. M. Cooper, M. Drobizhev, N. S. Makarov, A. Rebane, K. Y. Kim, R. Farley and K. S. Schanze, *Inorg. Chem.*, 2007, **46**, 6483–6494.
24 J. B. Pollock, T. R. Cook, G. L. Schneider, D. A. Lutterman, A. S. Davies and P. J. Stang, *Inorg. Chem.*, 2013, **52**, 9254–9265.
25 T. Lazarides, T. M. McCormick, K. C. Wilson, S. Lee, D. W. McCamant and R. Eisenberg, *J. Am. Chem. Soc.*, 2011, **133**, 350–364.
26 A. A. Rachford, S. Goeb and F. N. Castellano, *J. Am. Chem. Soc.*, 2008, **130**, 2766–2767.
27 (*a*) R. Ziessel and A. Harriman, *Chem. Commun.*, 2011, **47**, 611–631; (*b*) Z. Kostereli, T. Ozdemir, O. Buyukcakir and E. U. Akkaya, *Org. Lett.*, 2012, **14**, 3636–3639; (*c*) O. A. Bozdemir, S. Erbas-Cakmak, O. O. Ekiz, A. Dana and E. U. Akkaya, *Angew. Chem., Int. Ed.*, 2011, **50**, 10907–10912; (*d*) X. Zhang, Y. Xiao and X. Qian, *Org. Lett.*, 2008, **10**, 29–32; (*e*) J. Fan, M. Hu, P. Zhan and X. Peng, *Chem. Soc. Rev.*, 2013, **42**, 29–43; (*f*) X. Zhang, Y. Zeng, T. Yu, J. Chen, G. Yang and Y. Li, *J. Phys. Chem. Lett.*, 2014, **5**, 2340–2350.
28 M. T. Indelli, T. Bura and R. Ziessel, *Inorg. Chem.*, 2013, **52**, 2918–2926.
29 J. M. Keller and K. S. Schanze, *Organometallics*, 2009, **28**, 4210–4216.
30 W. Wu, J. Zhao, H. Guo, J. Sun, S. Ji and Z. Wang, *Chem.–Eur. J.*, 2012, **18**, 1961–1968.
31 W. Wu, H. Guo, W. Wu, S. Ji and J. Zhao, *J. Org. Chem.*, 2011, **76**, 7056–7064.
32 A. Loudet and K. Burgess, *Chem. Rev.*, 2007, **107**, 4891–4932.
33 G. Ulrich, R. Ziessel and A. Harriman, *Angew. Chem., Int. Ed.*, 2008, **47**, 1184–1201.

34 A. C. Benniston and G. Copley, *Phys. Chem. Chem. Phys.*, 2009, **11**, 4124–4131.
35 A. Kamkaew, S. H. Lim, H. B. Lee, L. V. Kiew, L. Y. Chung and K. Burgess, *Chem. Soc. Rev.*, 2013, **42**, 77–88.
36 S. G. Awuahab and Y. You, *RSC Adv.*, 2012, **2**, 11169–11183.
37 (*a*) Y. Yang, Q. Guo, H. Chen, Z. Zhou, Z. Guo and Z. Shen, *Chem. Commun.*, 2013, **49**, 3940–3942; (*b*) Y. Chen, J. Zhao, H. Guo and L. Xie, *J. Org. Chem.*, 2012, **77**, 2192–2206.
38 W. Wu, W. Wu, S. Ji, H. Guo, P. Song, K. Han, L. Chi, J. Shao and J. Zhao, *J. Mater. Chem.*, 2010, **20**, 9775–9786.
39 Y. Chen, J. Zhao, L. Xie, H. Guo and Q. Li, *RSC Adv.*, 2012, **2**, 3942–3953.
40 F. R. Dai, H. Zhan, Q. Liu, Y. Fu, J. Li, W. Wang, Z. Xie, L. Wang, F. Yan and W. Y. Wong, *Chem.–Eur. J.*, 2012, **18**, 1502–1511.
41 G. Zhou, W. Y. Wong, S. Y. Poon, C. Ye and Z. Lin, *Adv. Funct. Mater.*, 2009, **19**, 531–544.
42 J. S. Wilson, A. Köhler, R. H. Friend, M. K. Al-Suti, M. R. A. Al-Mandhary, M. S. Khan and P. R. Raithby, *J. Chem. Phys.*, 2000, **113**, 7627–7634.
43 K. S. Schanze, E. E. Silverman and X. Zhao, *J. Phys. Chem. B*, 2005, **109**, 18451–18459.
44 J. E. Rogers, T. M. Cooper, P. A. Fleitz, D. J. Glass and D. G. McLean, *J. Phys. Chem. A*, 2002, **106**, 10108–10115.
45 Y. Liu, S. Jiang, K. Glusac, D. H. Powell, D. F. Anderson and K. S. Schanze, *J. Am. Chem. Soc.*, 2002, **124**, 12412–12413.
46 T. M. Cooper, D. M. Krein, A. R. Burke, D. G. McLean, J. E. Rogers and J. E. Slagle, *J. Phys. Chem. A*, 2006, **110**, 13370–13378.
47 J. E. Haley, D. M. Krein, J. L. Monahan, A. R. Burke, D. G. McLean, J. E. Slagle, A. Fratini and T. M. Cooper, *J. Phys. Chem. A*, 2011, **115**, 265–273.
48 T. Lazarides, T. M. McCormick, K. C. Wilson, S. Lee, D. W. McCamant and R. Eisenberg, *J. Am. Chem. Soc.*, 2011, **133**, 350–364.
49 J. R. Lakowicz, *Principles of Fluorescence Spectroscopy*, Kluwer Academic, New York, 2nd edn, 1999.
50 B. Valeur, *Molecular Fluorescence: Principles and Applications*, Wiley-VCH Verlag: GmbH, 2001.
51 W. Wu, J. Zhao, J. Sun, L. Huang and X. Yi, *J. Mater. Chem. C*, 2013, **1**, 705–716.
52 C. Liao, J. E. Yarnell, K. D. Glusac and K. S. Schanze, *J. Phys. Chem. B*, 2010, **114**, 14763–14771.
53 A. A. Rachford, R. Ziessel, T. Bura, P. Retailleau and F. N. Castellano, *Inorg. Chem.*, 2010, **49**, 3730–3736.
54 M. Galletta, S. Campagna, M. Quesada, G. Ulrich and R. Ziessel, *Chem. Commun.*, 2005, 4222–4224.
55 M. Galletta, F. Puntoriero, S. Campagna, C. Chiorboli, M. Quesada, S. Goeb and R. Ziessel, *J. Phys. Chem. A*, 2006, **110**, 4348–4358.
56 W. Wu, L. Liu, X. Cui, C. Zhang and J. Zhao, *Dalton Trans.*, 2013, **42**, 14374–14379.
57 W. Wu, J. Sun, X. Cui and J. Zhao, *J. Mater. Chem. C*, 2013, **1**, 4577–4589.
58 J. Sun, F. Zhong, X. Yi and J. Zhao, *Inorg. Chem.*, 2013, **52**, 6299–6310.
59 J. S. Wilson, N. Chawdhury, M. R. A. Al-Mandhary, M. Younus, M. S. Khan, P. R. Raithby, A. Köhler and R. H. Friend, *J. Am. Chem. Soc.*, 2001, **123**, 9412–9417.
60 Y. Li, M. E. Köse and K. S. Schanze, *J. Phys. Chem. B*, 2013, **117**, 9025–9033.
61 C. Adamo and D. Jacquemin, *Chem. Soc. Rev.*, 2013, **42**, 845–856.
62 J. E. Yarnell, J. C. Deaton, C. E. McCusker and F. N. Castellano, *Inorg. Chem.*, 2011, **50**, 7820–7830.
63 W. Wu, H. Guo, W. Wu, S. Ji and J. Zhao, *Inorg. Chem.*, 2011, **50**, 11446–11460.
64 T. N. Singh-Rachford and F. N. Castellano, *Coord. Chem. Rev.*, 2010, **254**, 2560–2573.
65 J. Zhao, S. Ji and H. Guo, *RSC Adv.*, 2011, **1**, 937–950.
66 P. Ceroni, *Chem.–Eur. J.*, 2011, **17**, 9560–9564.
67 A. Monguzzi, R. Tubino, S. Hoseinkhani, M. Campione and F. Meinardi, *Phys. Chem. Chem. Phys.*, 2012, **14**, 4322–4332.
68 Y. C. Simon and C. Weder, *J. Mater. Chem.*, 2012, **22**, 20817–20830.
69 Y. Y. Cheng, T. Khoury, R. G. C. R. Clady, M. J. Y. Tayebjee, N. J. Ekins-Daukes, M. J. Crossley and T. W. Schmidt, *Phys. Chem. Chem. Phys.*, 2010, **12**, 66–71.
70 (*a*) S. Baluschev, V. Yakutkin, T. Miteva, Y. Avlasevich, S. Chernov, S. Aleshchenkov, G. Nelles, A. Cheprakov, A. Yasuda, K. Müllen and G. Wegner, *Angew. Chem., Int. Ed.*, 2007, **46**, 7693–7696; (*b*) S. M. Borisov, R. Saf, R. Fischer and I. Klimant, *Inorg. Chem.*, 2013, **52**, 1206–1216.
71 M. Haase and H. Schäfer, *Angew. Chem., Int. Ed.*, 2011, **50**, 5808–5829.
72 Q. Liu, T. Yang, W. Feng and F. Li, *J. Am. Chem. Soc.*, 2012, **134**, 5390–5397.
73 C. Zhang, J. Zheng, Y. Zhao and J. Yao, *Adv. Mater.*, 2011, **23**, 1380–1384.
74 W.-P. To, K. T. Chan, G. S. M. Tong, C. Ma, W.-M. Kwok, X. Guan, K.-H. Low and C.-M. Che, *Angew. Chem., Int. Ed.*, 2013, **52**, 6648–6652.
75 J.-H. Kang and E. Reichmanis, *Angew. Chem., Int. Ed.*, 2012, **51**, 11841–11844.
76 A. Nattestad, Y. Y. Cheng, R. W. MacQueen, T. F. Schulze, F. W. Thompson, A. J. Mozer, B. Fückel, T. Khoury, M. J. Crossley, K. Lips, G. G. Wallace and T. W. Schmidt, *J. Phys. Chem. Lett.*, 2013, **4**, 2073–2078.
77 T. F. Schulze, J. Czolk, Y.-Y. Cheng, B. Fückel, R. W. MacQueen, T. Khoury, M. J. Crossley, B. Stannowski, K. Lips, U. Lemmer, A. Colsmann and T. W. Schmidt, *J. Phys. Chem. C*, 2012, **116**, 22794–22801.
78 J. S. Lissau, J. M. Gardner and A. Morandeira, *J. Phys. Chem. C*, 2011, **115**, 23226–23232.
79 Q. Zhang, J. Li, K. Shizu, S. Huang, S. Hirata, H. Miyazaki and C. Adachi, *J. Am. Chem. Soc.*, 2012, **134**, 14706–14709.
80 S. Park, O. H. Kwon, Y. S. Lee, D. J. Jang and S. Y. Park, *J. Phys. Chem. A*, 2007, **111**, 9649–9653.
81 F. N. Castellano, I. E. Pomestchenko, E. Shikhova, F. Hua, M. L. Muro and N. Rajapakse, *Coord. Chem. Rev.*, 2006, **250**, 1819–1828.
82 H. Xiang, J. Cheng, X. Ma, X. Zhou and J. J. Chruma, *Chem. Soc. Rev.*, 2013, **42**, 6128–6185.

83 S. C. F. Kui, F.-F. Hung, S.-L. Lai, M.-Y. Yuen, C.-C. Kwok, K.-H. Low, S. S.-Y. Chui and C.-M. Che, *Chem.–Eur. J.*, 2012, **18**, 96–109.
84 P.-T. Chou, Y. Chi, M.-W. Chung and C.-C. Lin, *Coord. Chem. Rev.*, 2011, **255**, 2653–2665.
85 X. Xiong, F. Song, J. Wang, Y. Zhang, Y. Xue, L. Sun, N. Jiang, P. Gao, L. Tian and X. Peng, *J. Am. Chem. Soc.*, 2014, **136**, 9590–9597.